

Digitized by the Internet Archive
in 2012 with funding from
LYRASIS Members and Sloan Foundation

<http://archive.org/details/scanningelectron00coop>

SCANNING ELECTRON MICROSCOPE OBSERVATIONS OF
THE TRITICUM AESTIVUM:PUCCINIA
RECONDITA ASSOCIATION

by

DENNIS BLAKE COOPER

B.S., Biology, University of Southern Colorado, 1975

B.S., Chemistry, University of Southern Colorado, 1975

-

A MASTER'S THESIS

submitted in partial fulfillment of the

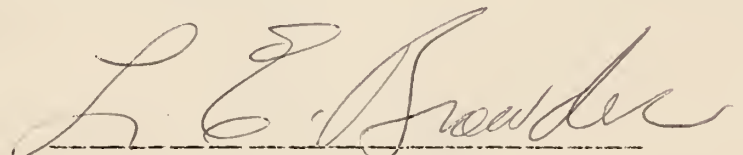
requirements for the degree

MASTER OF SCIENCE

Department of Plant Pathology

KANSAS STATE UNIVERSITY
Manhattan, Kansas
1979

Approved by:


Major Professor

Spec Coll:
 LD
 2665
 T4
 1979
 C66
 C.2

TABLE OF CONTENTS

	Page
List of Figures	ii
Acknowledgements	iii
Introduction	1
Chapter I - Evaluation of Several Techniques for SEM Observation of <u>Triticum aestivum</u> infected with <u>Puccinia recondita</u>	
Title	3
Abstract	4
Introduction	6
Materials and Methods	6
Results	10
Discussion	19
Literature Review	22
Chapter II - Ultrastructural Development of the <u>Triticum aestivum:Puccinia recondita</u> Association	
Title	25
Abstract	26
Introduction	27
Materials and Methods	28
Results	28
Discussion	38
Literature Review	41
Chapter III - Ultrastructural Modifications Associated with the Lrl0 Gene for Resistance to <u>Puccinia recondita</u>	
Title	44
Abstract	45
Introduction	46
Materials and Methods	47
Results	48
Discussion	52
Literature Review	58
Appendix A - Additional Scanning Electron Microscope Studies of <u>T. aestivum:P. recondita</u>	
	61
Appendix B - Ultraviolet Fluorescence Microscopy of <u>T. aestivum:P. recondita</u>	
	81

Appendix C - Transmission Electron Microscopy of
T. aestivum:P. recondita 90

Appendix D - Light Microscopy of
T. aestivum:P. recondita 93

Abstract

LIST OF FIGURES

	Page
Chapter I - Evaluation of Several Techniques for SEM Observation of <u>Triticum aestivum:Puccinia recondita</u>	
Effects of Fixation	12
Direct Observation Fig. 1	12
Lactophenol:Ethanol Fig. 2	12
Chloral hydrate Fig. 3	12
Standard fixation Fig. 4	12
Removal of Excessive Host Cytoplasm	14
Untreated control Fig. 5	14
Treated with 4% KOH Fig. 6	14
Resin-Embedding Technique	14
Air drying after etching Fig. 7	14
Freeze drying after etching Fig. 8	14
Wax-Embedding Technique Fig. 9	16
Examples of Correlated Observation	16
Transmission Electron Microscopy . Fig. 10	16
Light Microscopy Fig. 11	16
Ultraviolet Fluorescence Microscopy Fig.12	16
Chapter II - Ultrastructural Development of the <u>Triticum aestivum:Puccinia recondita</u> Association	
Germination - Penetration Phase	32
Germ tube development Fig. 1	32
Appressorium development Fig. 2	32
Intercellular Mycelial Phase	32
Young mycelia Fig. 3	32
Development of haustorial mother cells Fig. 4	32
Haustorial mother cell Fig. 5	32
Neck Scar in mother cell wall . . . Fig. 6	32
Haustorial Phase	32
Typical elongated haustoria Fig. 7	32
Non-median cross sections of mother cells and haustoria Figs. 8, 9	34
Invasion of host mesophyll cell . . Fig. 10	34

Invasion of host bundle-sheath cells	Fig. 11	34
Invagination of host plasmalemma	Fig. 12	34
Haustoria next to host nucleus	Figs. 13, 14	34
Sporulation Phase		36
Development of mycelial thallus	Figs. 15, 16	36
Development of urediospores and paraphyses	Fig. 17	36
Rupture of host epidermis	Fig. 18	36
Chapter III - Ultrastructural Modifications Associated with the Lrl0/Hpl0 Interaction in <u>Triticum aestivum:Puccinia recondita</u>		
Haustorial Development		50
LR:68A - High type	Fig. 1	50
TC:68A - High type	Fig. 2	50
LR:68B - Low type	Fig. 3	50
LR:68A - High type	Fig. 4	50
Haustorial Encasement	Fig. 5	50
Urediospore Development		50
Compressed urediospores in low type	Fig. 6	50
Normal urediospores in low type	Fig. 7	50
Urediospores in high type	Fig. 8	50
Appendix A - Additional Scanning Electron Microscopy Studies of <u>T. aestivum:P. recondita</u>		
		63
Appendix B - Ultraviolet Fluorescent Microscopy of <u>T. aestivum:P. recondita</u>		
		83
Appendix C - Light Microscopy of <u>T. aestivum:P. recondita</u>		
		91
Appendix D - Transmission Electron Microscopy of <u>T. aestivum:P. recondita</u>		
		94

ACKNOWLEDGEMENTS

I would like to acknowledge the Department of Plant Pathology, the Kansas Agricultural Experiment Station, and the U.S. Department of Agriculture for financial support as a graduate student and of this investigation.

I wish to thank Dr. Lewis E. Browder, for guidance, assistance, thought provoking discussions and his patient persistence in teaching me the art of reporting scientific research. I am also grateful for guidance from my advisory committee: Dr. A. S. Tomb, Dr. C. L. Kramer and Dr. A. Q. Paulsen.

Special thanks are given to John Krchma for his expertise with the SEM, to Dr. Larry Claflin for use of the Olympus BH microscope, and to Madelyn McArthur for computer type setting the thesis.

I am grateful to my parents for their never-ending support.

Most of all I am grateful to my loving wife for typing endless revisions and convincing me that I could accomplish this work.

INTRODUCTION

Throughout recorded history, men and nations, dependent upon cereal grains for a portion of their economic and food bases, have suffered the deprivations of reduced yield from cereal rust diseases. The exact nature of these diseases have only been understood for a relatively short time, and the study of the diseases has focused on preventing loss through resistance.

One of these diseases, wheat leaf rust, is the result of the Triticum aestivum L. em. Thell. : Puccinia recondita Rob. ex Desm. host:parasite association. Estimated annual losses to wheat leaf rust are about 1-2% of the total U.S. wheat crop, but in today's economy, the large acreages of wheat translate that small percentage into a sizeable economic loss. In 1979, wheat leaf rust caused an estimated 1.5% loss in Kansas wheat production. This 1.5% amounted to an estimated 5.78 million bushels of wheat valued at approximately 22.5 million dollars at the time of harvest.

The cytology and histology of T. aestivum:P. recondita have been studied with both the light and transmission electron microscopes, but until now no one has utilized the scanning electron microscope to observe this host:parasite association. Past studies have attempted to describe resistance mechanisms, however, experimental design did not include the use of a quadratic check to positively correlate observations to a specific gene pair. The objective of this

investigation was to more clearly establish the nature of the T. aestivum:P. recondita associations using the scanning electron microscope, as well as other methods of observation, giving particular attention to the hypersensitive reaction produced by the Lrl0/Lpl0 gene interaction.

During the investigation, the applicability of several preparative techniques for the histological study of this host:parasite combination were studied. In order to widely and quickly disseminate all the results of this investigation, the results are presented in journal article form. Therefore, the body of this thesis is comprised of three distinct journal articles, each written in the style and format of the journal for which it was intended to appear. Due to constraints on journal article length, several appendices have been added to contain the balance of the results. Appendix I contains additional observations made with the SEM. The remaining appendices contain observations with other methods including U. V. fluorescence-, light-, and transmission electron-, microscopy. The legends that appear on facing pages of the photographic plates give sufficient information to permit interpretation with minimal reference to the text. It is hoped that this format of organization will facilitate the use of this information by scholars who study this or related concerns in the future.

CHAPTER I

Evaluation of Several Techniques
for SEM Observation of
Triticum aestivum
infected with
Puccinia recondita

ABSTRACT

Several scanning electron microscope techniques were evaluated for suitability in studying the Triticum aestivum:Puccinia recondita association. The criteria for evaluation were simplicity, quality of preservation, amount of infected tissue exposed, and potential to correlate scanning electron microscope observations with light microscopy and transmission electron microscopy. Direct examination of fresh tissue was adequate for external structures only. In all other techniques, tissues were chemically fixed, dehydrated, and coated with gold-palladium prior to examination. Intercellular mycelium was shrunken in tissue fixed in either 1:2 lactophenol:ethanol or chloral hydrate, but such tissue also could be processed for examination with ultraviolet-fluorescence microscopy. Superior tissue preservation was accomplished with fixation in 3% acrolein-3% paraformaldehyde followed by 2% osmium tetroxide. Host cytoplasm often obscured the details of haustorial development within host cells. Treatment with 4% KOH removed host cytoplasm, but only a limited amount of tissue was exposed. More tissue was exposed by embedding in either Spurr's resin or Paraplast Plus, sectioning with a microtome, and removing the embeddment prior to observation. The resin-embedding technique completely removed host cytoplasm, but the host plasmalemma and various organelles

were retained with the wax-embedding technique. Both methods permitted correlated observation of the same tissue with other methods.

The cereal rusts have been studied extensively, because of their economic importance and an academic interest in the host:parasite associations formed. Man's first explanations of the cereal rust diseases were based on mythology; however, the advent of the light microscope revealed the true nature of host:parasite relationships involved (Allen 1923, 1927; Stakman 1915). The transmission electron microscope has greatly extended man's understanding of these diseases (Bracker and Littlefield 1973). The scanning electron microscope has helped establish the distribution and physical relationships of parasitic fungi within host tissue, including a recent study of the Triticum aestivum:Puccinia graminis associations (Plotnikova et al. 1979). A better understanding of biological systems is often obtained when observations by several methods are correlated. Such a correlated approach is particularly useful when studying the interaction between two organisms. Examination of one tissue sample by several methods was deemed important in establishing the nature of the host:parasite association in the T. aestivum:P. recondita system. The purpose of this investigation was to evaluate several preparative techniques for SEM observation of that system.

MATERIALS AND METHODS

Week old seedlings of wheat (Triticum aestivum L. em Thell.) were dip inoculated with urediospores of Puccinia

recondita Rob. ex Desm. (Browder 1971). Uninoculated seedlings were maintained as controls. At 24-hour intervals, 3 to 14 days after inoculation, 0.5 cm² sections were taken 2 cm below the apex of primary leaves and prepared for examination with an ETEC Autoscan scanning electron microscope (ETEC Corp., Haywood, CA 94545). Electron images were recorded on Polaroid P/N 55 type film.

Direct Examination. Leaf tissue was examined directly, without chemical fixation or metallic coating (Day and Scott 1973). Tissue sections were mounted on aluminum stubs with silver-collodion. The cut ends of the sections were also sealed with silver-collodion to minimize dehydration during examination. The electron beam was operated at 5 KV acceleration potential, while scanning the specimen, to reduce the amount of charging. A 10-20 KV potential was used for exposing photographs once an area of interest was located. All operations were done quickly to minimize tissue damage.

Chemical Fixation. Leaf tissue was fixed by one of three methods. In the first two methods, tissue was fixed overnight in either 1:2 lactophenol:ethanol or chloral hydrate. In the third method, which will be referred to as the standard fixation schedule, tissue was fixed in 3% acrolein--3% paraformaldehyde in a 0.1M phosphate buffer (pH 7.0, containing a drop of 0.02% Triton X-100) for 3-6 hr at 25 C. The fixative was perfused into the tissue by applying a light vacuum. After three 15 min rinses and an overnight

rinse in buffer the tissue was postfixed for 3-6 hr in 2% OsO_4 in the same buffer at 4 C.

After fixation, tissue was rinsed three times in buffer and dehydrated in a graded ethanol series (50, 75, 90, 95, 2 x 100%, 15 min per step), followed by a graded ethanol-amylacetate series. Dehydrated tissue was CO_2 critical-point dried (Anderson 1951) in a Denton DCP-1 critical-point dryer (Denton Vacuum, Inc., Cherry Hill, NJ 08003). Tissue sections were attached to aluminum stubs with silver-collodion, leaving the cut ends exposed. The tissue was lightly carboned and then vapor coated with gold-paladium in a Kinney vacuum evaporator.

Host Cytoplasm Removal. A portion of the material processed by the standard fixation schedule was resectioned with a razor blade in preparation for host cytoplasm removal (Kinden and Brown 1975). In this method bound osmium was first removed from the resectioned surface by treating tissue in 1.0% aqueous periodic acid for 2 min, prior to cytoplasm removal with 4% aqueous KOH for 30 min at 55 C. After washing for 5 min in 1% acetic acid and 1 hr in distilled water, the tissue was rehardened in buffered 2% OsO_4 at 4 C for 6 hr. An attempt to shorten Kinden and Brown's method by eliminating the periodic acid treatment and using tissue that was not post-fixed in OsO_4 was unsuccessful.

Resin Embedding. After standard fixation and dehydration, leaf tissue was infiltrated with a graded

series of Spurr's low viscosity epoxy resin (formulation A, medium-firm, Spurr 1969). When infiltration was complete (24 hr), the tissue was flat embedded in fresh resin and cured at 70 C and -1 atm for 48 hr. Embedded tissue was trimmed and sectioned with glass knives on a Richert OM-2 ultramicrotome (William J. Hacker and Co., West Caldwell, NJ). Monitor sections (8-10 um) were stained in 1% Toluidine Blue and examined with an Olympus BH microscope. Thin (90-100 nm) silver-gold sections were collected on 100 mesh hexagonal copper grids (Ted Pella Co., Box 510, Tustin, CA 92680). that had been filmed with paralodion and lightly carboned. Grids were stained for 25-30 min each in 5% uranyl-acetate in 50% ethanol (Watson 1958) and lead citrate (Reynolds 1963) prior to examination with a Phillips 201 transmission electron microscope. The remaining block-face was treated with 2.5% sodium-ethoxide to etch the resin away from the tissue (Pring 1975). The blocks were washed extensively in 100% ethanol and then either air-, critical-point-, or freeze-dried; mounted on aluminum stubs with cement, sputter coated and examined with the SEM.

Wax Embedding. Tissue was fixed in 3% acrolein-3% paraformaldehyde according to the standard fixation schedule, but was not post-fixed in OsO₄, prior to dehydration and infiltration with Paraplast Plus (Fisher Scientific Co.) and cast into blocks. The tissue was sectioned with a hand operated microtome (Baush and Lomb). Serial sections were collected for light microscopy, and the

paraffin was removed from the remaining tissue block with xylene prior to dehydration, critical-point drying, vapor coating and observation (Precheur 1977).

U. V. Fluorescence. Tissue that was fixed in either 1:2 lactophenol:ethanol or chloral hydrate could also be examined with U. V. fluorescence prior to SEM observation. The method was the same as reported by Rohringer et al., 1977, except Tinopal UNPS was substituted for Calcoflour 2MR New (J. R. Tomerlin, personal communication). Tissue was examined with an Olympus BH microscope equipped for epifluorescence. Generally, two BG-12 exciter filters and a heat filter were used in conjunction with the B dichroic mirror, and an 0-530 barrier filter. Images were recorded on black and white Kodak brand Tri-X panatomic film, ASA 400(6).

RESULTS

Scanning electron micrographs of tissue prepared by the techniques evaluated are shown in Figs. 1-9. The scale bar inserted in the lower right corner of each figure represents 10 mm.

Direct examination of tissue with the SEM is shown in Fig. 1. Note presence of a crystalline-wax lattice on the host cuticle. Figs. 2-4 demonstrate the quality of preservation obtained with chemical fixation in: 1:2 lactophenol:ethanol, chloral hydrate, and the standard fixation schedule, respectively. Note the shrinkage of

mycelium in Figs. 2 and 3 as compared with the superior preservation in Fig. 4. Host cytoplasm covering a haustorium is shown in Fig. 5. Fig. 6 shows a second haustorium after removal of host cytoplasm with 4% KOH. Examples of the resin-embedding technique are shown in Figs. 7 and 8. Fig. 7 is a good example of tissue that was air-dried after etching, and Fig. 8 is an example of tissue freeze-dried after etching. In both cases, note the removal of the host cytoplasm and plasmalemma. Fig. 9 is an example of the wax-embedding in which the host plasmalemma is retained intact.

Fig. 10 is a transmission electron micrograph of resin embedded material. Fig. 11 is a thick section from resin-embedded tissue stained in 1% Toluidine Blue and examined with an Olympus BH microscope. Fig. 12 is tissue treated with Tinopal UNPS and examined with Olympus BH microscope equipped for epifluorescence.



Fig. 1. Observation of fresh uncoated tissue. Note the crystalline-wax lattice covering the host epidermis and stoma (S). Also note the germinating urediospore. Scale bar = 10 um.

Fig. 2. Tissue fixed in 1:2 lactophenol:ethanol. Note the shrinkage of the fungal mycelium (M). Scale bar = 10 um.

Fig. 3. Tissue fixed in chloral hydrate. Mycelium (M) is shrunken, while haustorial mother cells are not. Scale bar = 10 um.

Fig. 4. Tissue fixed by the standard fixation schedule. Mycelium (M) and haustorial mother cells without shrinkage. Scale bar = 10 um.

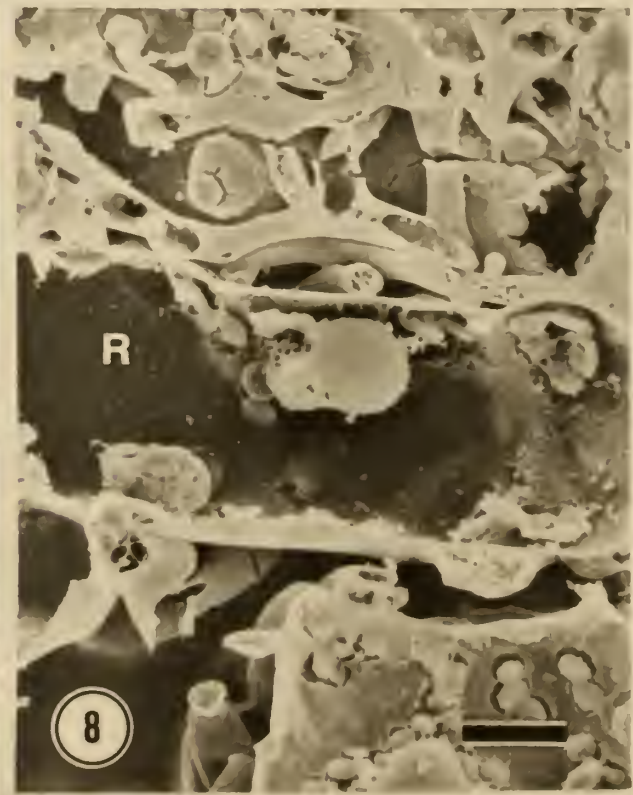
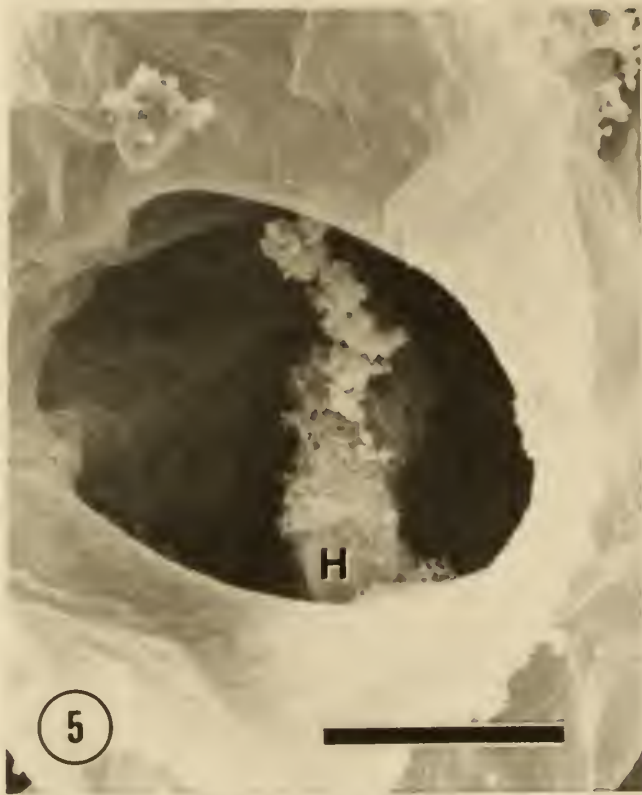


Fig. 5. Tissue fixed by the standard fixation schedule, in which host cytoplasm conceals the details of the haustorium (H). Scale bar = 10 um.

Fig. 6. Tissue treated with 4% KOH after standard fixation to remove excessive host cytoplasm from haustorium (H). Scale bar = 10 um.

Fig. 7. Optimal results obtainable with the resin-etch technique followed by air-drying. Note the haustoria (H) and the sectioned haustorial mother cell (arrow). Undissolved resin (R) partially fills the infected host cell and lightly coats the tissues. Standard fixation schedule. Scale bar = 10 um.

Fig. 8. Resin-etch technique followed by freeze-drying. This method permitted more complete removal of resin (R) from the host:parasite interface. Standard fixation. Scale bar = 10 um.

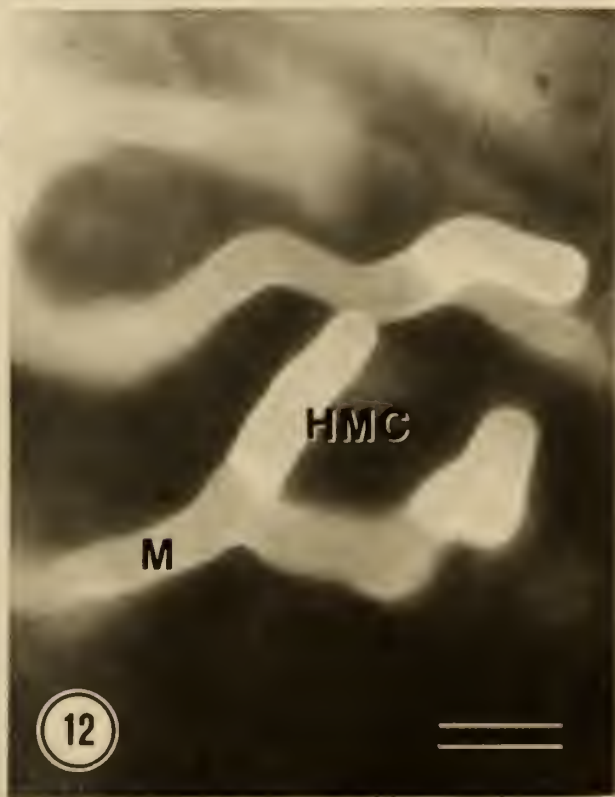
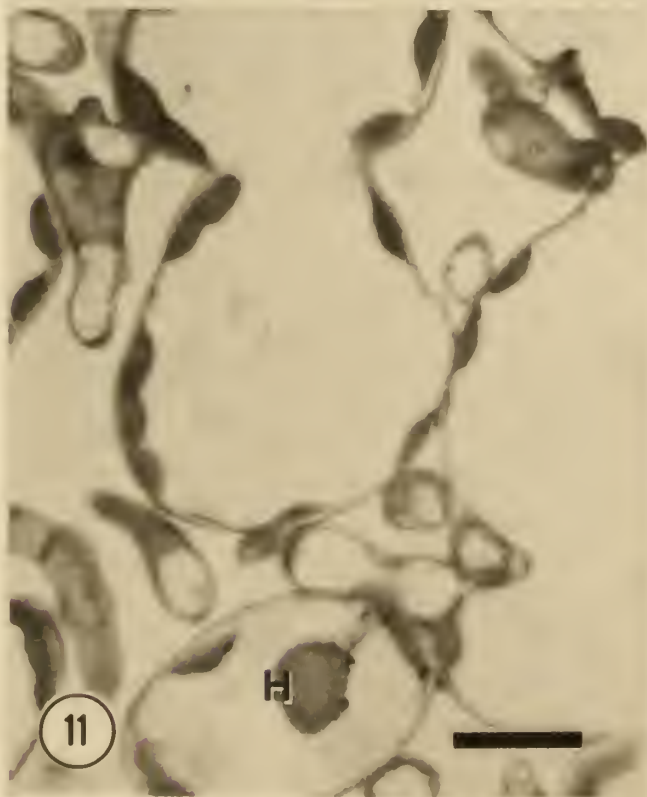
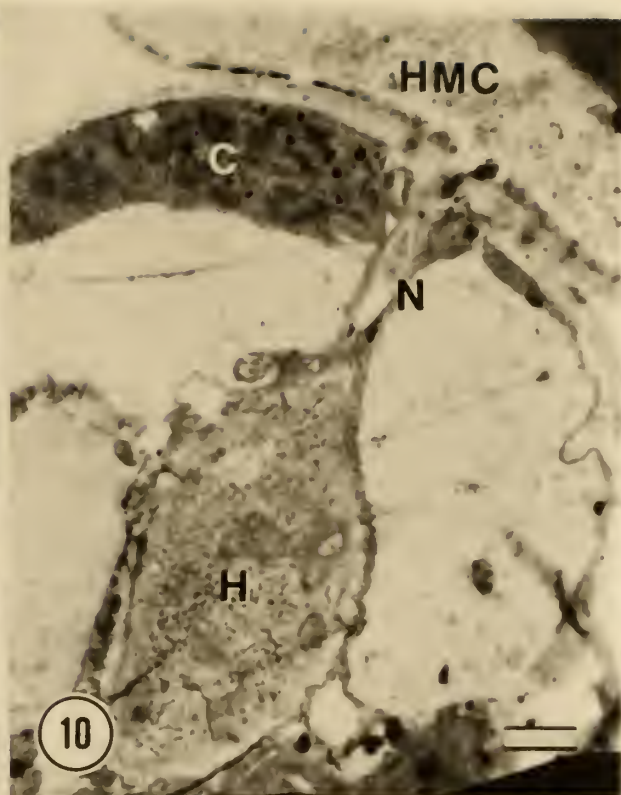
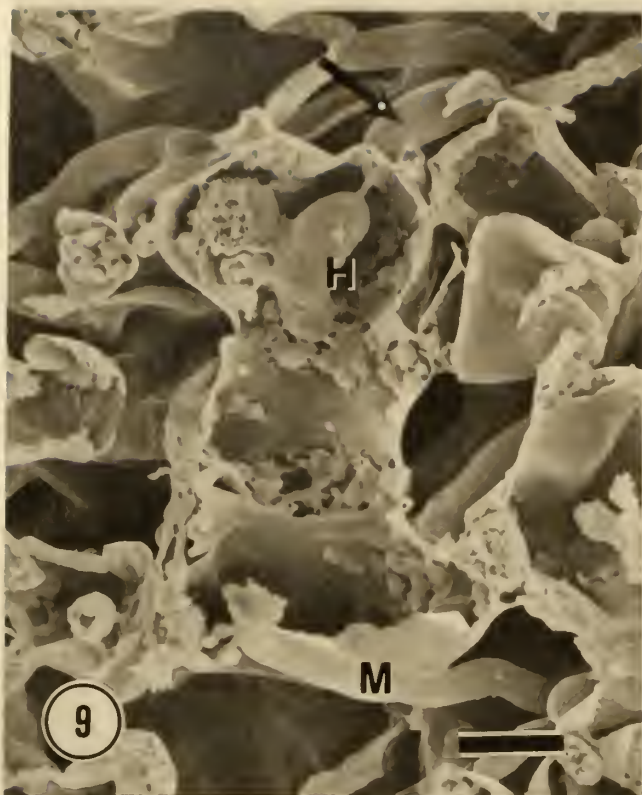


Fig. 9. Wax-etch technique. The embedment has been completely removed, to clearly show intracellular mycelium (M), a haustorial mother cell (arrow) which is connected to a haustorium (H). The host cytoplasm and organelles (nucleus and chloroplasts) are retained with this method. Standard fixation. Scale bar = 10 um.

Fig. 10. Correlated observation with TEM. Tissue was processed with standard fixation schedule, embedded in Spurr's resin, thin sectioned, stained 30 mins. each in uranyl acetate and lead citrate prior to observation with a Phillips 201 transmission electron microscope. Note the haustorial mother cell (HMC) connected to the haustorium (H) by the haustorial neck (N). Also note the host chloroplast (C). Scale bar = 1 um.

Fig. 11. Correlated observation with light microscopy, of 10 um sections of resin embedded tissue stained in 1% toluidine blue. Haustorium (H) stained dark. Scale bar = 10 um.

Fig. 12. Correlated observation with U. V. fluorescence. Tissue fixed in 1:2 lactophenol:ethanol, and stained with Tinopal UNPS. Haustorial mother cells (HMC) stained more intensely than mycelium (M). Haustoria did not stain. Scale bar = 10 um.

DISCUSSION OF CHAPTER I

DISCUSSION

Several methods for preparing plant tissue for SEM observation have recently been developed (Echlin 1974). The use of several of these techniques to study T. aestivum:P. recondita associations helped to identify infection structures and locate artifacts of fixation and handling. All the methods evaluated proved useful in observation of some of the fungal structures.

Direct observation of tissue was adequate only for external structures during primary infection or uredium development during advanced stages of the disease (Fig. 1). Specimens could only be observed for short periods of time (1-5 min) before the electron beam, high vacuum, and localized charging produced artifacts. The crystalline-wax lattice of the host cuticle was retained with this method, but removed in tissue that was fixed and critical-point dried.

Fixation with 1:2 lactophenol:ethanol (Fig. 1) or chloral hydrate (Fig. 2) followed by dehydration, critical-point drying and vapor coating permitted observation of subepidermal fungal infection structures, including intercellular mycelium, haustorial mother cells, and uredium development. Mycelium was shrunken in such tissue; however, mother cells retained a smooth appearance, possibly due to thicker cell walls. These methods also had the advantage of correlation with U. V. fluorescence (Fig. 12).

The standard fixation schedule resulted in superior tissue preservation as noted by the absence of mycelial shrinkage (Fig. 4). The improved preservation is probably due to the hardening effects of the OsO_4 .

Excessive amounts of host cytoplasm often obscured details of haustoria, within host cells (Fig. 5). Removal of host cytoplasm with 4% KOH permitted observation of haustoria without interference (Fig. 6). The harsh chemical treatments involved in this technique may introduce artifacts, and were also time consuming. The amount of subepidermal tissue that could be exposed was still a limiting factor.

The resin embedding technique exposed more internal infection structures including non-median sections of haustoria revealing the neck connections between haustorial mother cells and haustoria (Fig. 7). The extent of resin removal was difficult to control. Insufficient removal of resin left infection structures indistinct, and excessive removal often caused tissue to collapse during air-drying. CO_2 critical-point drying was attempted to prevent tissue collapse, but the resin blocks were shattered by pressure differentials within the bomb. Freeze-drying of etched resin blocks produced excellent results (Fig. 7). The majority of the host cytoplasm was removed with this method. Despite the harsh nature of the sodium ethoxide treatment, artifacts were minimal when the degree of etching was correct. This method is somewhat involved; however, it has

the advantage of correlation with TEM (Fig. 10), and the light microscope (Fig. 11).

The host plasmalemma was retained with the wax-embedding technique as an invaginated sheath or covering over the haustoria (Fig. 9). This condition has been described with the T. aestivum:P. graminis association (Plotnikova et al. 1979). The potential for correlation with light microscopy, large amounts of tissue exposed, the quality of preservation, and relative simplicity of this method, seem to make it the method of choice for this particular situation.

One technique not evaluated in this study was freeze-fracturing of tissue (Plotnikova et al. 1979). It has the distinct advantages of exposing large amounts of interior tissue, fractured along the natural (varied) plane of the host:parasite interface, with minimal preparation. The resin and wax-embedding techniques, although requiring more preparation, are both capable of exposing large areas sectioned on an exact plane, and have the potential to correlate SEM results with other methods of observation.

REFERENCES

1. ALLEN, R. F. 1923. A cytological study of infection of Baart and Kanred wheats by *Puccinia graminis triticii*. *J. Agric. Res.* 23:131-152.
2. ALLEN, R. F. 1927. A cytological study of orange leaf rust, *Puccinia triticina* physiologic form II, on Malakoff wheat. *J. Agric. Res.* 34:697-714.
3. ANDERSON, T. F. 1951. Techniques for the preservation of three dimensional structure in preparing specimens for electron microscope. *Trans. N. Y. Acad. Sci., Ser. II.* 13:130-134.
4. BRACKER, C. E. and L. J. LITTLEFIELD. 1973. Structural concepts of host pathogen interfaces. Pages 159-318. in eds. R. J. W. Byrde and C. V. Cutting. Academic Press, New York, NY. 499 p.
5. BROWDER, L. E. 1971. Pathogenic specialization in cereal rust fungi, especially *Puccinia recondita* f. sp. *tritici*: Concepts, methods of study, and application. Technical Bulletin 1432. USDA.
6. COOPER, D. B. 1979. Scanning electron microscope observations of the *Triticum aestivum*:*Puccinia recondita* association. Appendix B. M.S. Thesis, Kansas State University, Manhattan, KS 66506.
7. DAY, P. R. and K. J. SCOTT. 1973. Scanning electron microscopy of fresh material of *Erysiphe graminis* f. sp. *hordei*. *Physiol. Plant Path.* 3:433-435.

8. ECHLIN, P. 1974. The application of scanning electron microscopy and X-ray microanalysis in the plant sciences. A bibliography in scanning electron microscopy/1974 (Part II). Proceedings of the workshop on scanning electron microscopy and the plant sciences. IIT Research Institute, Chicago, IL 60616. USA.
9. KINDEN, D. A. and M. F. BROWN. 1975. Technique for scanning electron microscopy of fungal structures within plant cells. *Phytopathology* 65:74-76.
10. PLOTNIKOVA, Y. M., L. J. LITTLEFIELD, and J. D. MILLER. 1979. Scanning electron microscopy of the haustorium-host interface regions in wheat infected with *Puccinia graminis* f. sp. *tritici*. *Physiol. Plant Path.* 14:37-39.
11. PRECHEUR, R. J. 1977. The effects of wind and wind plus sand on tomatoes. (*Lycopersicon esculentum* L.) PhD. Thesis, Kansas State University, Manhattan, KS 66506.
12. PRING, R. J. 1975. Scanning electron microscopy of rust haustoria. *J. Micros.* 103:289-291.
13. REYNOLDS, E. G. 1963. The use of lead citrate at high pH as an electron opaque stain in electron microscopy. *J. Cell Biol.* 17:208-212.
14. ROHRINGER, R.; W. K. SIM; D. J. SAMBORSKI; and N. K. HOWES. 1977. Calcofluor: An optical brightener for

- fluorescence microscopy of fungal plant parasites in leaves. *Phytopathology*. 67:808-810.
15. SPUR, A. J. 1969. A low-viscosity epoxy resin embedding medium for electron microscopy. *J. Ultrastructure Res.* 26:31-43.
 16. STAKMAN, E. C. 1915. Relation between *Puccinia graminis* and plants highly resistant to its attack. *J. Agric. Res.* 4:193-199.
 17. TOMERLIN, J. R. (personal communication concerning the use of Tinopal UNPS as an optical brightener) Dept. Plant Pathology, Kansas State University, Manhattan, KS 66506.
 18. WATSON, M. L. 1958. Staining of tissue sections for electron microscopy with heavy metals. *J. Biochem. Biophys. Cytol.* 4:475-478.

CHAPTER II

Ultrastructural Development of the
Triticum aestivum:Puccinia recondita
Association

ABSTRACT

COOPER, D. B. 1980. Ultrastructural development of the Triticum aestivum:Puccinia recondita association.

Wheat, Triticum aestivum, was inoculated with urediospores of Puccinia recondita. Samples of infected tissue were prepared for the scanning electron microscope 3-14 days after inoculation. Germ tubes developed from germinating urediospores and elongated perpendicular to the host vascular system. The host was invaded after appressoria formed over host stomata. An intercellular mycelium was established with haustorial mother cells at the apices of the mycelium. Circular neck scars seen in mother cells corresponded in size and location to the haustorial necks. During early stages of infection, haustoria invaded host mesophyll cells; later host bundle sheath cells were also infected. The host plasmalemma was invaginated around the haustoria which were frequently in close proximity to host nuclei. A thallus developed beneath the host epidermis 5-9 days after inoculation. A uredium developed from this thallus. Urediospores were initially ovate and smooth and became spherical and covered with spines at maturity.

Additional keywords: Wheat leaf rust, cytology and histology, host:parasite associations.

INTRODUCTION

The cytology and histology of the host:parasite associations involved in cereal rusts have been studied extensively because of economic importance of the diseases and an academic interest in the nature of host:parasite associations formed. These studies have usually sought to explain resistance mechanisms and varietal response to infection.

The infection cycles and epidemiology of the rust diseases of wheat have been described in detail (12). The wheat stem rust association of Triticum spp.:Puccinia graminis have received particular attention, including light microscopy by Allen (1) and Stakman (15) during the early 1900's; however, the Triticum spp.:Puccinia recondita association has been studied less extensively (2).

Transmission electron microscope studies have greatly extended our understanding of rust fungi and other obligate parasites which form haustoria. Bracker and Littlefield (3) have reviewed the literature of transmission electron microscope examination of host:parasite associations. More recently, the scanning electron microscope (SEM) has helped establish the distribution and physical relationships of fungi within host tissues, including recent studies of P. graminis f. sp. triticii by Plotnikova et al. (14) and Melampsora lini by Hassan and Littlefield (8). Echlin (7) has reviewed SEM literature pertinent to the plant sciences.

The objective of this investigation was to establish the nature of the T. aestivum:P. recondita association using the SEM.

MATERIALS AND METHODS

Wheat (Triticum aestivum L. em Thell.) cultivar Thatcher *6/Exchange, RL6004, was seeded in 7.6 cm diameter pots in the greenhouse. This host line contains the Lr10 gene for reaction to P. recondita Rob. ex Desm. (6). Wheat seedlings (7 days old) were dip inoculated (4) with urediospores of culture isolate UN01-68A, ATCC PR67, of Puccinia recondita Rob. ex Desm. The use of another host cultivar ('Thatcher', CI 10003) and/or parasite culture isolate (UN01-68B, ATCC PR51) to describe ultrastructural development of that association are noted where applicable in the results section. Uninoculated seedlings were maintained as controls. Leaf tissue was removed at 24 hr intervals, 3-14 days after inoculation. Tissue sections (0.5 cm²) were prepared by one of several methods reported previously (5, Chap. I) prior to examination with an ETEC Autoscan SEM (ETEC Corp., 3392 Investment Blvd., Haywood, CA 94545).

RESULTS

The scanning electron micrographs in Figs. 1-17 are representative of the T. aestivum:P. recondita association studied. The host cultivar Thatcher *6/Exchange with Lr10,

and the parasite culture UN01-68A, with Hnl0, are represented unless specifically noted otherwise. The differences in ultrastructural development and resistance mechanisms noted with various host cultivars and/or parasite cultures are reported in a separate paper (5, Chap. III).

Germ tubes and appressoria had formed over host stoma prior to the observation of tissue 3 days after inoculation with urediospores. Germ tubes frequently elongated perpendicular to the host vascular system, which increased the probability of eventual contact with a them. However, failure to elongate toward nearby stomata indicated that germ tubes were not chemotropically attracted toward stomata. Direction of germ tube elongation changed when the apex contacted host trichomes, necrotic host epidermal cells, other germ tubes, or urediospores (Fig. 1). Appressoria developed in the depressions in the host epidermis surrounding stomata. The appressoria were often seen to have finger-like attachments to the stomatal guard cells (Fig. 2). These finger-like attachments can also be seen with ultraviolet fluorescence microscopy (5, Appendix B).

Subepidermal intercellular mycelium was formed after stomatal penetration. This mycelium was typically 2.5-3.5 μ m in diameter and branched extensively through host tissue (Figs. 3,4). Haustorial mother cells formed from swollen apices of the intercellular mycelium and were delimited from the mycelium by a septum (Figs. 4,5). Proximal to the

haustorial mother cells, the mycelium developed one or two branches which continued to elongate and subsequently form additional haustorial mother cells. The haustorial mother cells were 4-4.5 μm in diameter and 8-10 μm in length.

Hhaustorial mother cells were frequently seen to exhibit circular neck scars (0.35 to 0.45 μm in diameter) which corresponded in size and location with the area in which the host cell wall was penetrated (Fig. 5). The scars had a fibrillar network present which appeared continuous with the inner wall layers of the haustorial mother cell, with outer layers forming the circumference of the pore (Fig. 6). Once the host cell wall was penetrated, an elongated haustorial neck was formed which was attached to a haustorium within the host cell.

Numerous haustoria and non-median sections of haustoria that revealed neck connections between haustorial mother cells and haustoria (Figs. 7-9) were exposed. The diameters of haustorial necks and the pores found in the mother cells were approximately equal. Haustoria invaded host mesophyll cells during early stages of the infection period and continued until uredium formation. Host bundle sheath cells were invaded during later stages of the infection period prior to uredium formation. On occasion, host epidermal cells were invaded by haustoria. The haustoria were typically elongate in form (Fig. 7). Some haustoria were capitate or globose with finger-like projections attached to the main body of the haustorium (Figs. 8,9). In some

cases, individual host cells were invaded by 2 or more haustoria (Fig. 9). Haustoria initially invaded host mesophyll cells (Fig. 10), and later invaded host bundle-sheath cells (Figs. 8,11)). The host plasmalemma was invaginated to form a covering over the developing haustoria (Fig. 12).

Haustoria were often found in close proximity or direct contact with host nuclei (Figs. 12,13,14). The nuclear envelope appeared atrophied at the site of direct contact with the haustorium (Fig. 14).

From 5 to 9 days after inoculation, a thallus developed between the host epidermis and mesophyll cells. This fungal thallus was so tightly compacted that cell walls of individual hyphae became fused together (Fig. 15). Short urediophores and elongated paraphyses developed perpendicularly to the thallus (Figs. 15,16). The urediospores that developed from the swollen tips of the urediophores were initially ovate in shape and had only partially developed spines. Fully developed urediospores were roughly spherical in shape and were uniformly ornamented with spines (Fig. 17). The developing uredium ruptured the host epidermis 7 to 10 days after inoculation, releasing the mature urediospores (Figs. 17,18)).

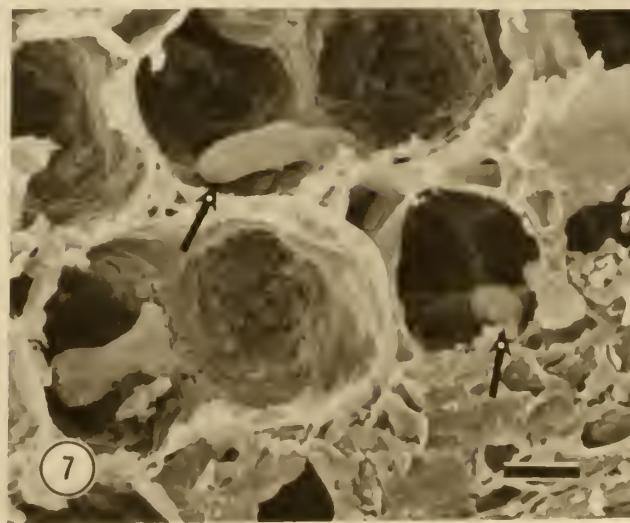
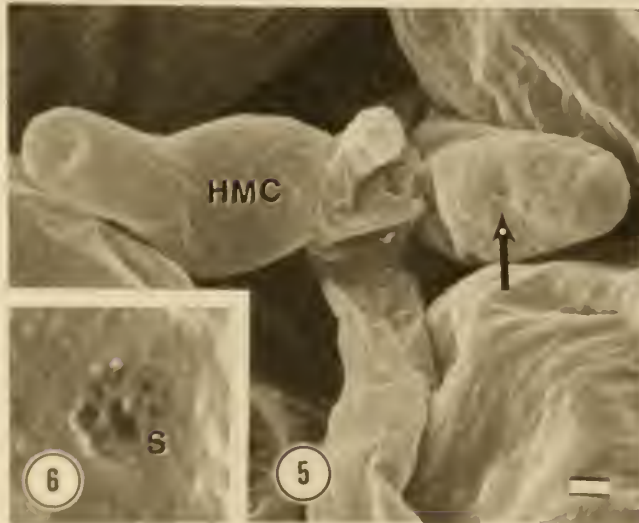
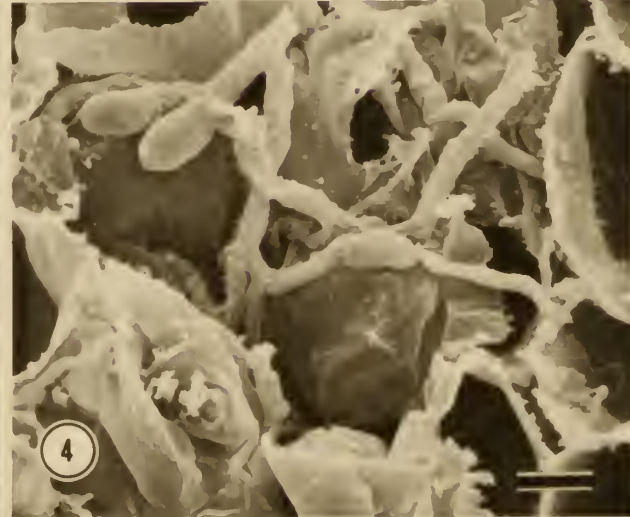
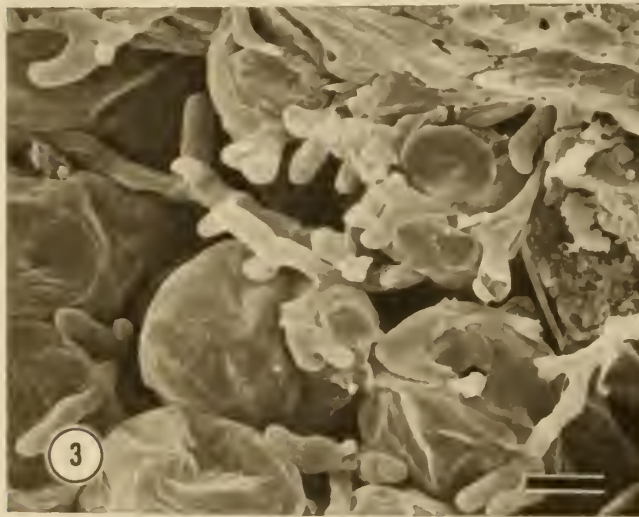
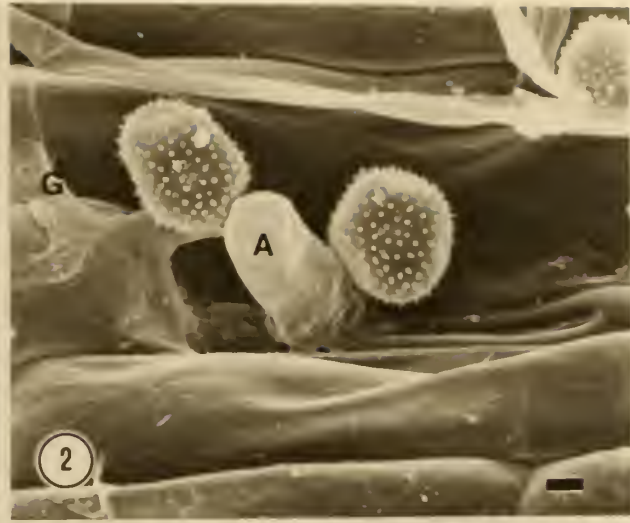
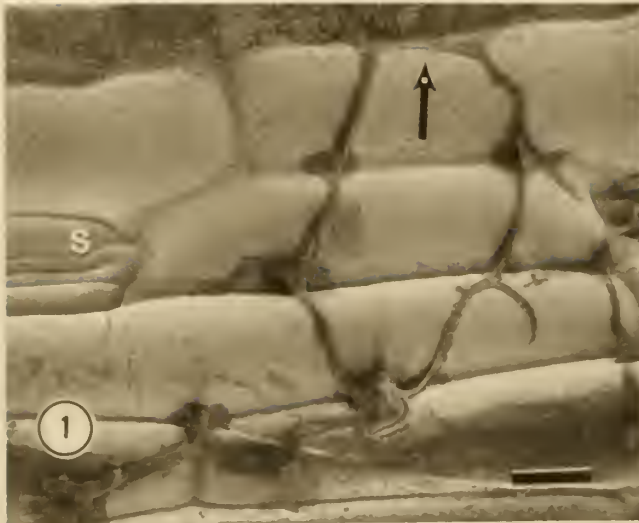


Fig. 1. A germinating urediospore in which the germ tube tended to elongate perpendicularly to the host vascular system, in response to the crystalline-wax lattice of the host cuticle. The germ tube turned around when it lost orientation with the crystalline-wax lattice at a necrotic host cell (arrow), passed near a host stoma (S) without turning toward it, and lost orientation again when it contacted the remnants of the urediospore.

Fig. 2. A germ tube (G) that located the depression around a host stoma and formed an appressorium (A) with small finger-like attachments to the guard cells.

Fig. 3. Development of intercellular mycelium (2.5-3.5 μm in diameter) that branched extensively.

Fig. 4. Development of haustorial mother cells at the apices of intracellular mycelium.

Fig. 5. An enlargement of Fig. 4. Showing a haustorial mother cell (HMC) delimited from the mycelium by a septum. A second haustorial mother cell has a scar (arrow) where the haustorial neck was severed during preparation.

Fig. 6. An enlargement of the neck scar (S) 3.5 μm in diameter. Note the fibrillar network continuous with the inner wall layers of the mother cell with the outer wall layers forming the circumference of the scar.

Fig. 7. Development of typical elongate haustoria (arrows).

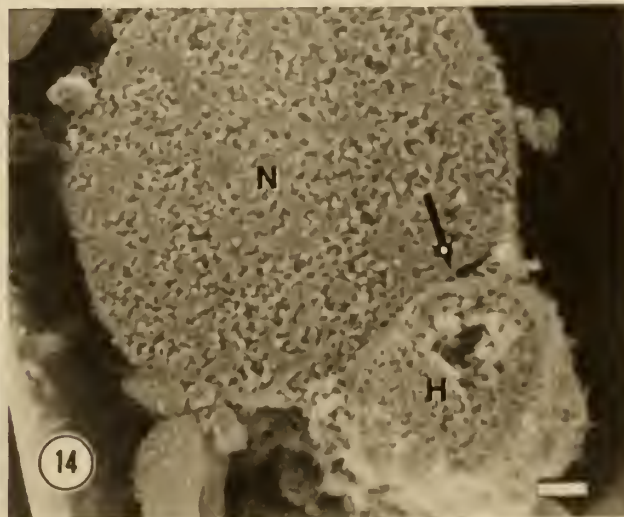
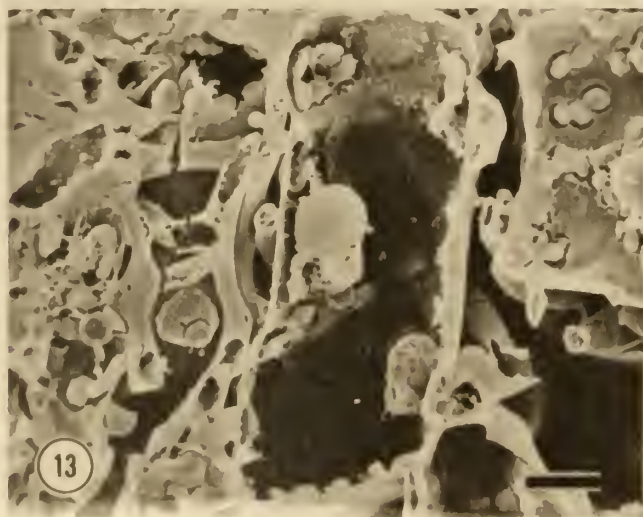
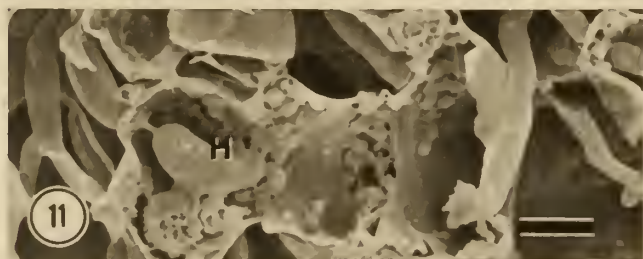
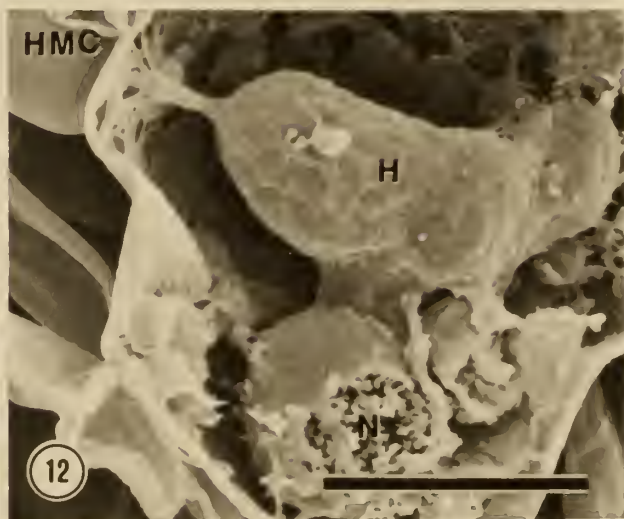
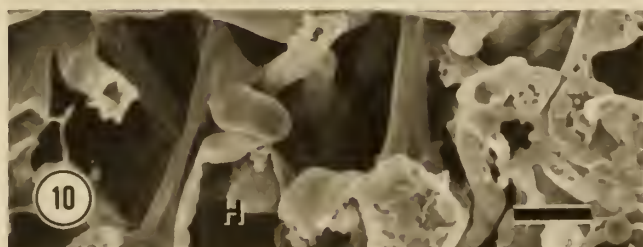


Fig. 8. A near-median section through a haustorial mother cell (arrow) and a capitate haustorium (H) with finger-like projection. The host bundle sheath cell at upper right is infected with a typical elongate haustorium (H).

Fig. 9. A single host cell invaded by two haustoria. Note the neck connection between the haustorium (H) and the haustorial mother cell (HMC).

Fig. 10. A host mesophyll cell infected with a haustorium (H).

Fig. 11. A host bundle sheath cell infected with a haustorium (H).

Fig. 12. An enlargement of Fig. 11. The host plasmalemma is invaginated to form a sheath around the haustorium (H) and the haustorial neck connection to the haustorial mother cell (HMC). The haustorium is also in close proximity to a partially sectioned host nucleus (N).

Fig. 13. A cross-section through a haustorium in direct contact with a host nucleus.

Fig. 14. An enlargement of Fig. 13. The host nucleus (N) is atrophied (arrow) at the site of direct contact with the haustorium (H).

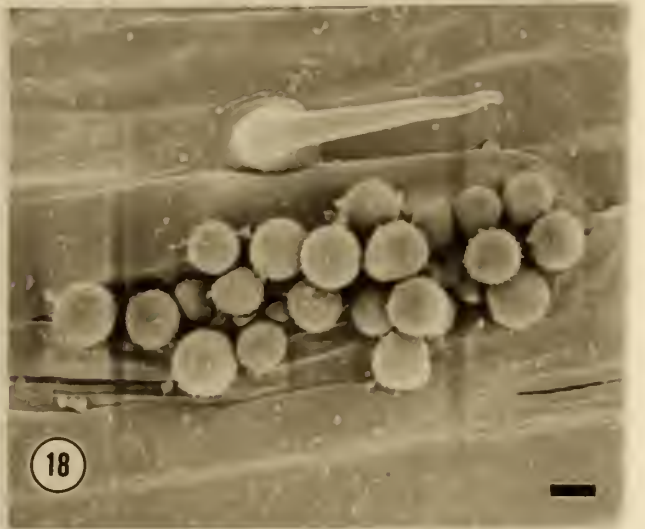
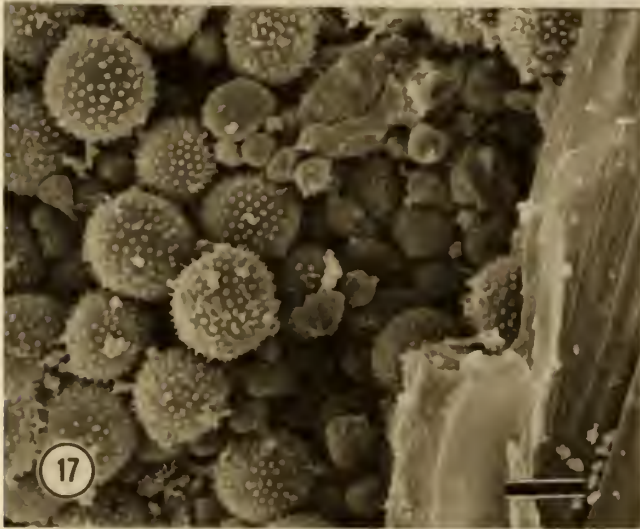
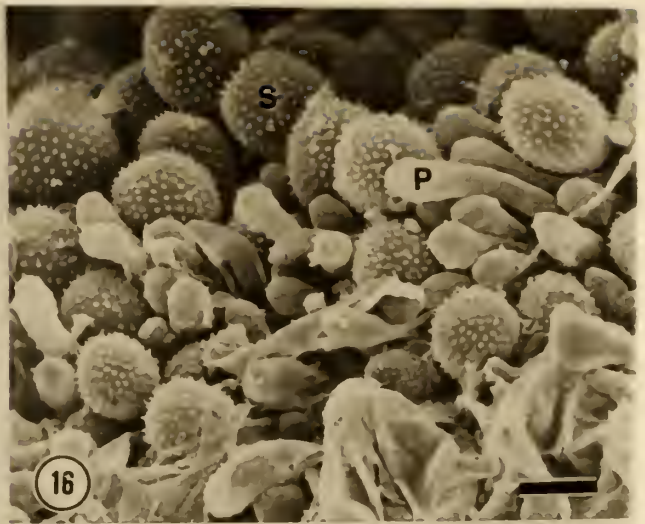
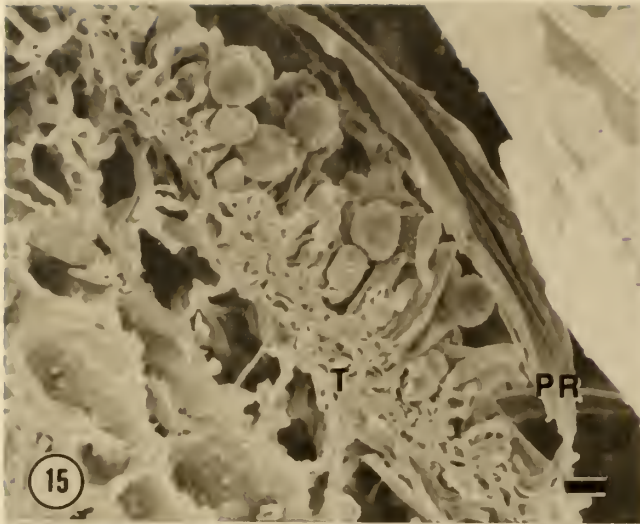


Fig. 15. The development of a thallus (T) beneath a uredium. Paraphyses and urediophores develop perpendicular to this mycelial thallus. The entire uredium is separated from the host epidermis by a thin peridium (PR).

Fig. 16. Paraphyses (P) elongated past the developing urediospores which were initially ovate with small spines but matured to spherical well-spined urediospores (S).

Fig. 17. A uredium with urediospores at various stages of development. The ruptured host epidermis is to the right.

Fig. 18. A top view of a young uredium beginning to rupture the host epidermis. The pointed structure above the uredium is a host trichome.

DISCUSSION

The development of germ tubes perpendicular to the vascular system maximized the probability of germ tubes eventually contacting a stoma. This phenomenon has been described with T. aestivum:P. graminis (9) as a thigmotropic response to the crystalline-wax lattice on the wheat cuticle. Temporary loss of contact with the crystalline lattice also explains why germ tubes develop lateral attachments at the folds in the cuticle between epidermal cells, and become disoriented after contacting necrotic host cells, trichomes, and urediospores (Fig. 1).

The fact that germ tubes do not necessarily elongate toward the nearest stoma, and often pass near a stoma without turning toward it, indicate that stomatal stimuli have little effect on germ tube orientation. Once a germ tube contacts the depression in the epidermis surrounding a stoma, an appressorium is formed. The finger-like attachments to the guard cells may provide an anchor for the appressoria during host penetration (Fig. 2).

Mycelium that develops following host penetration has a similar branching pattern and size distribution to mycelium of P. graminis (14). Haustorial mother cells appear to develop from hyphal apices only after contact with host cell walls, suggesting that some form of host:parasite recognition may be operating at this stage of the infection cycle. The haustorial mother cells are composed of several distinct wall layers and are less prone to shrinkage due to

fixation and handling than the intercellular mycelium (5).

TEM examination of other host:parasite associations (3) has revealed that the innermost wall layer of the haustorial mother cell is continuous with the initial portion of the haustorial neck. The diameters of the pores and haustorial necks are similar. Pores may be seen most frequently when host tissues are manually dissected to expose more tissue prior to metallic coating. This causes the haustorial mother cells to be separated from host cells at the delicate neck region, leaving a neck scar on the haustorial mother cell walls (Figs. 5,6). The presence of the fibrillar matrix in the haustorial neck region of the haustorial mother cells has not been reported in other host:parasite combinations and may be unique to this system. Alternately, the matrix observed in these studies may have been remnants of fungal cytoplasm within the haustorial mother cell.

Recently, Plotnikova et al. (14) have confirmed earlier work (10) demonstrating that the host plasmalemma is not ruptured by the invading haustorium of P. graminis, but rather becomes invaginated to form a covering over the haustorium and its sheath. The results of this study confirm that this condition also exists in tissue infected with P. recondita (Fig. 12).

Developing haustoria often occur in close proximity or direct contact with host nuclei. Nuclear envelopes appear atrophied at the site of direct contact with the haustorium (Fig. 7), which may be one reason why host cells often

become necrotic after infection. Haustoria have been seen in close proximity to host nuclei in other host:parasite associations, including Linum usitatissimum:Melampsora lini (11) and T. aestivum:Puccinia striiformis (13).

Mares (13) reported increased numbers of starch grains in chloroplasts of wheat infected with P. striiformis using TEM. I observed no such differences in chloroplasts of control and inoculated seedlings with the SEM in this study.

While the host may be adversely affected by any number of responses to infection (necrosis, loss of metabolites, chlorosis, etc.), increased evapotranspiration due to uredium formation plays a substantial role in crop losses from wheat leaf rust (12). Hassan and Littlefield (8) have described uredium development in L. usitatissimum:M. lini. This study indicates urediospore development of P. recondita appears similar to M. lini. The confirmation of these similarities will require transmission electron microscopy. Paraphyses tend to elongate beyond developing urediospores and thus appear to play an important part in rupturing the host epidermis. Paraphyses may also have secondary functions as they remain intact after the host epidermis is broken.

In summary, the SEM has proven useful in confirmation and clarification of the ultrastructural development of the T. aestivum:P. recondita association.

LITERATURE CITED

1. ALLEN, R. F. 1923. A cytological study of infection of Baart and Kanred wheats by *Puccinia graminis tritici*. J. Agric. Res. 23:131-152.
2. ALLEN, R. F. 1927. A cytological study of orange leaf rust, *Puccinia triticina* physiologic form II, on Malakoff wheat. J. Agric. Res. 34:697-714.
3. BRACKER, C. E. and L. J. LITTLEFIELD. 1973. Structural concepts of host pathogen interfaces. Pages 159-318. in eds. R. J. W. Byrde and C. V. Cutting. Academic Press, New York, NY. 499 p.
4. BROWDER, L. E. 1971. Pathogenic specialization in cereal rust fungi, especially *Puccinia recondita* f. sp. tritici: Concepts, methods of study, and application. Technical Bulletin 1432. USDA.
5. COOPER, D. B. 1979. Scanning electron microscope observations of the *Triticum aestivum*:*Puccinia recondita* association. M. S. Thesis, Kansas State University, Manhattan, KS 95 p.
6. DYCK, P. L. and E. R. KERBER. 1971. Chromosome locations of three genes for leaf rust resistance in common wheat. Can. J. Gen. Cytol. 13:480-483.
7. ECHLIN, P. 1974. The application of scanning electron microscopy and X-ray microanalysis in the plant sciences. Bibliography in scanning electron

- microscopy 1974 (Part II). Proceedings of the workshop on scanning electron microscopy and the plant sciences.
8. HASSAN, Z. M. and L. J. LITTLEFIELD. 1979. Ontogeny of the uredium of *Melampsora lini*. *Can. J. Bot.* 57:639-649.
 9. LEWIS, B. G. and J. R. DAY. 1972. Urediospore germ-tubes of *Puccinia graminis tritici* in relation to the time structure of wheat leaf surfaces. *Trans. Br. mycol. Soc.* 58:139-145.
 10. LITTLEFIELD, L. J. and C. E. BRACKER. 1970. Continuity of host plasma membrane around haustoria of *Melampsora lini*. *Mycologia* 62:609-614.
 11. LITTLEFIELD, L. J. and C. E. BRACKER. 1972. Ultrastructural specialization at the host-pathogen interface in rust-infected flax. *Protoplasma* 74:271-305.
 12. LOEGERING, W. Q.; J. W. HENDRIX, and L. E. BROWDER. 1967. The rust diseases of wheat. *Agriculture Handbook No. 334.* 22 p. USDA.
 13. MARES, D. J. 1979. A light and electron microscope study of the interaction of yellow rust (*Puccinia striiformis*) with a susceptible wheat cultivar. *Ann. Bot.* 43:183-189.
 14. PLOTNIKOVA, Y. M., L. J. Littlefield, and J. D. Miller. 1979. Scanning electron microscopy of the haustorium-host interface regions in wheat infected

- with *Puccinia graminis* f. sp. *tritici*. *Physiol. Plant Path.* 14:37-39.
15. STAKMAN, E. C. 1915. Relation between *Puccinia graminis* and plants highly resistant to its attack. *J. Agric. Res.* 4:193-199.

CHAPTER III

Ultrastructural Modifications

Associated with the

Lr10/Lp10

Interaction in

Triticum aestivum:Puccinia recondita

ABSTRACT

COOPER, D. B. 1980. Ultrastructural Modifications Associated with the Lr10/Lpl0 Interaction in Triticum aestivum:Puccinia recondita.

Two lines of wheat Triticum aestivum were inoculated with two cultures of Puccinia recondita. This formed a quadratic check that produced three high infection types and one low infection type (IT). Samples from each of the four host:parasite combinations were examined with a scanning electron microscope. Differences between the infection types were largely quantitative rather than qualitative. Haustoria in high ITs were typically elongate. The high types also had an extensively developed mycelium and produced large numbers of well-developed urediospores. Low IT haustoria were typically capitate, or with a digitate lobe. The low IT also had smaller mycelium colonies and produced fewer urediospores than high types. Haustoria developing in the host line with Lr10 were infrequently encased with an apposition produced by the host. In one instance, urediospores were compressed in the low IT.

Additional keywords: Wheat leaf rust, hypersensitivity, scanning electron microscope, resistance.

Because of their economic importance, the cereal rusts have been studied extensively. Generally, such studies have sought to explain resistance mechanisms and varietal response to infection.

The Triticum spp.:Puccinia graminis associations have received particular attention, including light microscopy by Allen (1) and Stakman (20). The cytology and histology of Triticum spp.:Puccinia recondita associations have been studied less extensively (2).

As early as 1902, Ward (21) observed a correlation between resistance to infection and necrosis of host mesophyll cells in the Bromus spp.:Puccinia dispersa (=Bromus:P. recondita) association. After discovering a similar condition with Triticum spp.:P. graminis, Stakman (20) concluded that "after entrance, the fungus rapidly kills a limited number of the plant cells" and "after having killed the host cells in its immediate vicinity, seems unable to develop further." This rapid host cell necrosis was termed 'hypersensitivity.' This mechanism is still widely used to explain incompatibility in many host:parasite associations. Stakman further concluded that "relations between plant and parasite in partially resistant and almost totally immune plants are different in degree only." Despite its widespread acceptance, the entire concept has recently been questioned (4,12,16).

The gene-for-gene hypothesis (8) provides the basis for utilizing a quadratic check (18) which is essential for the

study of host:parasite gene pair interactions.

The purpose of this study was to examine the ultrastructure of the low IT produced by the Lr10/Lp10 interaction of T. aestivum:P. recondita using the scanning electron microscope (SEM).

MATERIALS AND METHODS

The wheat (Triticum aestivum L. em Thell.) cultivar 'Thatcher', CI 10003, and a near-isogenic line Thatcher *6/Exchange, RL6004, which contains the Lr10 gene for reaction (6), were planted in 7.6 cm diameter pots in the greenhouse. Thatcher and the near-isogenic line will be referred to here as TC and LR, respectively. Week-old seedlings of the two wheat lines were dip inoculated with two urediospore cultures of Puccinia recondita Rob. ex Desm., and subsequently placed in a moist chamber at 15 C and 100 RH for 12 hr (3). Uninoculated seedlings of each line were maintained as controls. The two urediospore cultures, UN01-68A (ATCC PR67) and UN01-68B (ATCC PF51), which will be referred to here as 68A and 68B, have Hr10 and Lp10, respectively, when paired with the Lr10 host gene for resistance. The inoculated wheat formed a quadratic check (18) as summarized below:

LR:68A, Lr10:HP10 = High Infection Type

LR:68B, Lr10:Lp10 = Low Infection Type

TC:68A, Hr10:Hp10 = High Infection Type

TC:68B, Hr10:Lp10 = High Infection Type

At 24 hr intervals, 3-14 days after inoculation, 0.5 cm² sections were taken 2 cm below the apex of primary leaves, fixed in acrolein-3% paraformaldehyde at 25°C for 3-6 hr, followed by 2% OsO₄ at 4°C for 3-6 hr, before additional processing as previously reported (5) for examination with an ETEC Autoscan SEM (ETEC Corp., 3392 Investment Blvd., Hayward, CA 94545).

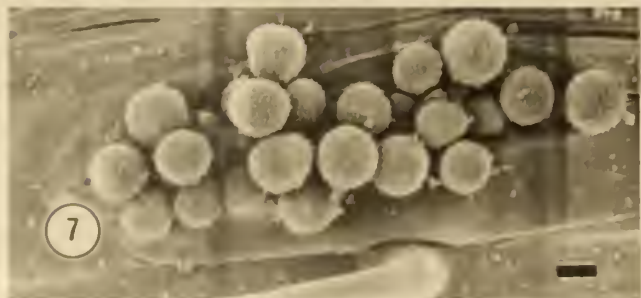
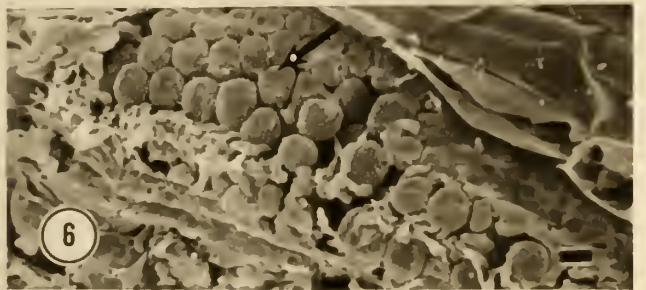
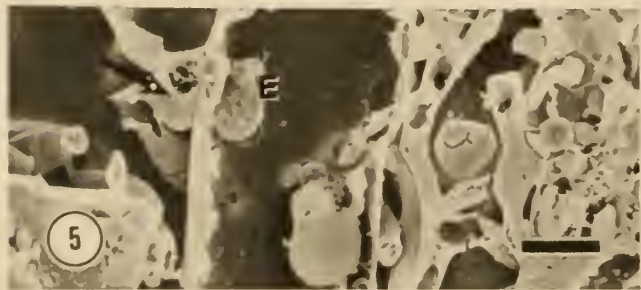
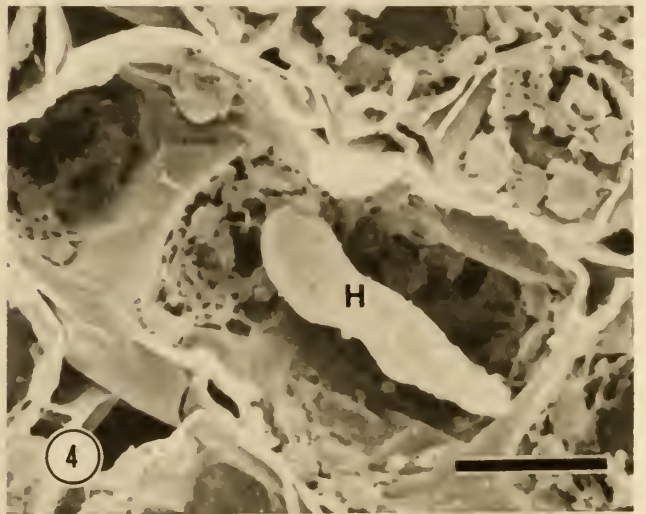
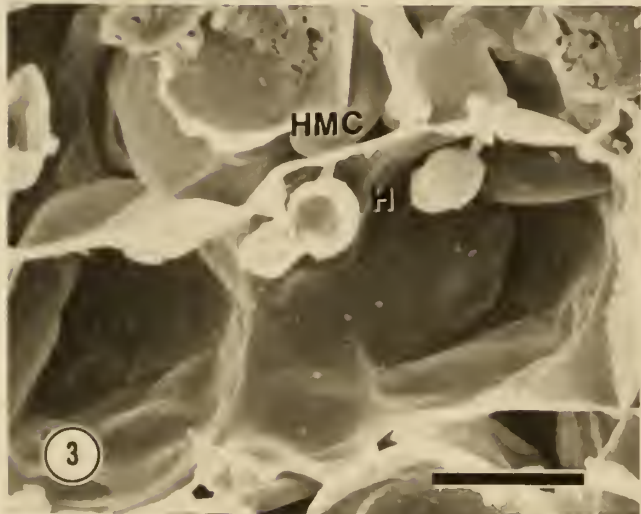
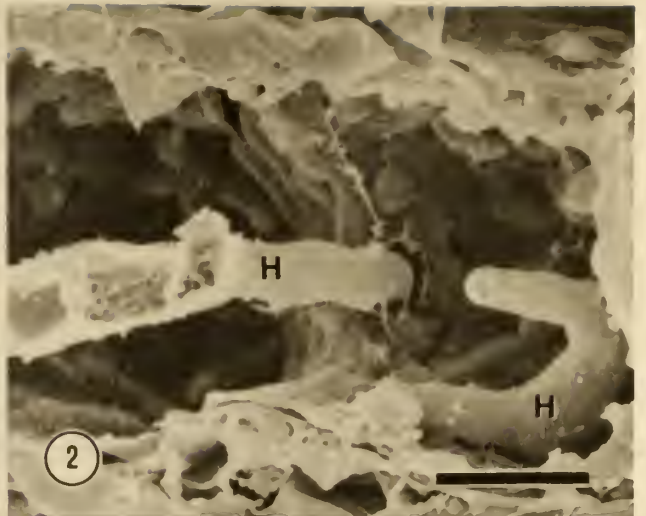
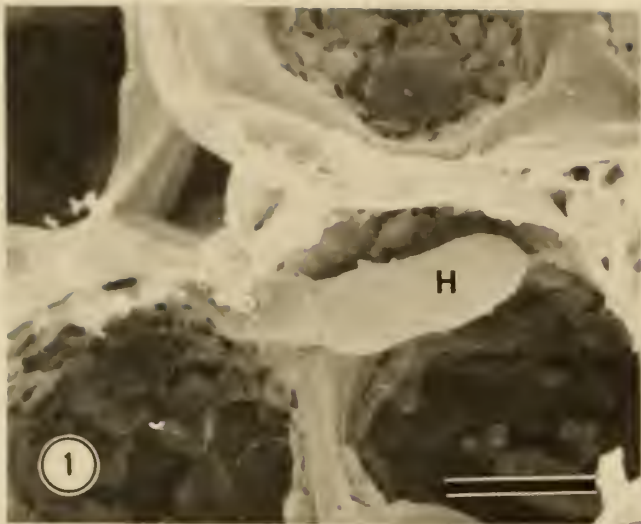
RESULTS

The differences between the high and low ITs were largely quantitative. The portion of the infection cycle from urediospore germination to host penetration was identical in all four host:parasite combinations, insofar as I observed.

The most significant qualitative histopathological difference between the infection types was the development of haustoria. In high infection types (LR:68A, TC:63A, TC:63B) haustoria were typically extended or elongate in form and showed no restriction of development (Figs. 1,2,4). Low infection type (LR:68B) haustoria were typically capitate in form; some had a digitate projection attached (Fig. 3). Infrequently, an encasement (surrounding a haustorium) adjacent to a haustorial mother cell was present in the host line with Lrl0 (Fig. 5).

Quantitative differences in the infection types included more extensive mycelium development and urediospore production in the high IT than in the low IT. In one case,

the urediospores produced in the low IT (LR:68B) appeared compressed as a result of increased difficulty in rupturing the host epidermis (Fig. 6). Generally, however, urediospores produced in the low IT (Fig. 7) were indistinguishable from urediospores in the high ITs (Fig. 8).



Figs. 1-4. Haustoria in the four host:parasite combinations of the quadratic check. All four were prepared by the same methods, 7 days after inoculation. The scale bar represents 10 um in all figures. Fig. 1. Elongated haustoria (H) produced by LR:68A, the haustorial neck is at the right of the haustorium. Fig. 2. Elongated haustoria (H) produced by TC:68A. Fig. 3. Small capitate haustoria (H) produced by LR:68B, connected to haustorial mother cells (HMC) by a narrow haustorial neck. The section plane passed through the haustorium on the left which had a digitate projection. Elongated haustoria (H) produced in TC:68B. Fig. 4.

Fig. 5. The presence of an encasement (E) (surrounding a haustorium) adjacent to a haustorial mother cell (arrow) with the LR:68A combination. Such encasements were noted infrequently in both the LR:68A and LR:68B combinations.

Fig. 6. Compression of urediospores (arrow) in the low infection type LR:68B due to increased difficulty in rupturing the host epidermis.

Fig. 7. Urediospore production in the LR:68B combination. The urediospores were identical to those produced in the high infection type combinations but were fewer in number.

Fig. 8. Urediospore production in the TC:68B combination.

DISCUSSION

Haustorium development was the only consistent qualitative difference between high and low ITs. Haustoria in the high IT associations (LR:68A, TC:68A, TC:68B) were extended or elongate in form and showed no restriction of development (Figs. 1,2,4). Low IT (LR:68B) haustoria were typically capitate in form; some had a digitate projection (Fig. 3). Capitate haustoria in the low IT demonstrate that the host is capable of some form of parasite recognition followed by an active response that alters development of the haustoria. The use of the quadratic check established that the 68B culture was capable of producing high IT haustoria when associated with a host that lacks specific reaction genes to that culture (i.e., TC:68B). Mares (15) has suggested a reduction in the amounts or types of metabolites accumulated by the parasite prior to sporulation, in low infection types of T. aestivum:P. striiformis. The constriction of haustorium development in the low IT in this study may be related to a reduction in metabolic reserves.

Heath and Heath (10) describe a "dimorphic immune reaction" in Vigna sinensis:Uromyces phaseoli association in which the host cells either become necrotic or form a callose sheath or encasement around invading haustoria. A similar condition is described with T. aestivum:P. graminis (7), in which a lomosome forms in apposition to developing haustoria. Occasionally (Fig. 5), the presence of an

encasement (surrounding a haustorium) was noted adjacent to a haustorial mother cell. This may be one example of how multiple resistance mechanisms effect the 'degrees of sensitivity' expressed by the various infection types. Stakman's (20) hypothesis that host:parasite relations in partially resistant and totally immune plants differ in degree only is based on the premise that the rate and intensity of host cell necrosis produces distinct degrees of sensitivity. I believe that differences in high and low infection types are the cumulative product of all the host:parasite gene interactions involved in the association, rather than a "degree only" condition based solely on hypersensitivity. This position is supported by Heath and Heath (10), who propose that infection type is the result of a complex series of events during the infection process with each individual host:parasite interaction constituting a 'switching point' between susceptibility and resistance. Johnson et al. (11) have proposed that a similar condition exists in the Hordeum vulgare:Evrysiphe graminis association.

These proposals are consistent with the gene-for-gene relationship established by Flor (8) in the Linum ussitatissimum:Melampsora lini association, and Person's (17) extension of that work into a model system for host:parasite associations in general.

Loegering (14) calls the infection type the 'phenotypic expression' of the host:parasite genotypes involved, and

proposes the term 'aegricorpus' to describe the "single living manifestation of specific genetic interactions in and between the host and pathogen." The aegricorpus simultaneously expresses host resistance/susceptibility, parasite virulence/avirulence, and environmental effects. The host and parasite interact to form in effect a 'third entity,' representative of the genotypes involved. Though the term aegricorpus itself has not been used extensively to describe this condition, it is apparent that necrotic host cells can best be explained as a consequence of the specific interaction of host:parasite gene pairs and the environment.

Stakman's (20) original explanation of resistance of wheat to infection by P. graminis is based on hypersensitive host cell necrosis, and states that a relationship exists between the extent and rate of parasite development and the presence of necrotic host cells. If this is the case, an obligate parasite's development would soon be arrested when host cell necrosis becomes more rapid than colonization by the parasite. Sharp and Emge (19) have demonstrated that the parasite is not completely inactivated. They found in some cases, that when tissue from a necrotic lesion of Triticum spp.:P. graminis was transplanted into a susceptible host, active mycelium and a typical high IT was formed.

In the low IT (LR:68B), the fungal mycelium did not infect as extensive an area of the host, as in the three

high IT associations. However, mycelium present in the low IT type did not appear morphologically different from mycelium in the high IT associations. The low infection type produces a limited amount of sporulation (Figs. 6,7), which would not be expected if parasite development is inactivated by host cell necrosis.

The low IT has more necrotic host cells near the site of infection than high types, thus the Lrl0 gene has been categorized as expressing hypersensitivity. Brown et al. (4) question the entire concept of hypersensitivity, arguing that just as mycelial growth is limited as a consequence of incompatibility, host cell necrosis may in fact be a consequence rather than the cause of incompatibility. Other studies (4,12,16) indicate that hypersensitivity may not be the only factor in producing the low reaction to infection, or that diverse mechanisms are involved (13).

Heath (9) has noted that even though hypersensitive cell necrosis may not be the primary determinant of resistance, it still must have some effects on the IT observed. Indeed, to discount such effects would be as incorrect as to assume that they are the sole cause of resistance.

In one instance, the urediospores in the low IT were compressed into cubicle shapes (Fig. 6). This may be the result of increased difficulty in rupturing the host epidermis by a smaller mycelial thallus with fewer urediospores and paraphyses. Generally the urediospores

produced in the low IT (even though less numerous) are morphologically indistinguishable from those produced by the high ITs.

The differences in development in high and low infection types are not solely due to a lack of ability on the part of the parasite or the presence of a specific resistance mechanism on the part of the host. Such differences are the result of a complex series of interactions between the host, parasite, and environment.

Results of SEM observation demonstrate that a classic case of hypersensitivity, as originally defined by Stakman (20), is not caused by the gene pair tested, even though increased host cell necrosis is present. This statement is based on the following observations of the low IT. Mycelia in the low IT are not inactivated and develop sufficiently to support limited amounts of sporulation. An incompatible reaction in haustorium development is noted in the low IT which could partially account for quantitative differences between the high and low IT's. Additionally, haustorial encasements indicate that multiple mechanisms of incompatibility may be present. These factors imply that a series of compatible/incompatible host:parasite interactions are involved in determining the infection type observed. In keeping with the gene-for-gene hypothesis, each specific interaction would be conditioned by a specific gene pair of the host:parasite association. The cumulative effects of these interactions prevent the parasite from producing an

extensive mycelial thallus and large numbers of urediospores, while changing infection structures only slightly.

These findings are valid only for the host:parasite gene pair tested, and may not be typical of all low ITs within the T. aestivum:P. recondita association. Even though evidence indicates that hypersensitivity may not be the primary determinant of incompatibility with the gene pair tested, it does not imply that this phenomenon is not present in other host:parasite associations which effect resistance.

LITERATURE CITED

1. ALLEN, R. F. 1923. A cytological study of infection of Baart and Kanred wheats by *Puccinia graminis triticici*. *J. Agric. Res.* 23:131-152.
2. ALLEN, R. F. 1927. A cytological study of orange leaf rust, *Puccinia triticina* physiologic form II, on Malakoff wheat. *J. Agric. Res.* 34:697-714.
3. BROWDER, L. E. 1971. Pathogenic specialization in cereal rust fungi, especially *Puccinia recondita* f. sp. *tritici*: Concepts, methods of study, and application. Technical Bulletin 1432. USDA.
4. BROWN, J. F.; W. A. SHIPTON, and N. H. WHITE. 1966. The relationship between hypersensitive tissue and resistance in wheat seedlings infected with *Puccinia graminis tritici*. *Ann. Appl. Biol.* 58:279-290.
5. COOPER, D. B. 1979. Scanning electron microscope observations of the *Triticum aestivum*:*Puccinia recondita* association. Chapter I. M.S. Thesis. Kansas State University, Manhattan, KS 66506.
6. DYCK, P. L. and E. R. KERBER. 1971. Chromosome locations of three genes for leaf rust resistance in common wheat. *Can. J. Gen. Cytol.* 13:480-483.
7. ERLICH, M. A.; J. F. SCHAFER; and H. G. ERLICH. 1968. Lomasomes in wheat leaves infected by *Puccinia graminis* and *P. recondita*. *Can. J. Bot.* 46:17-20.

8. FLOR, H. H. 1956. The complementary genic systems of flax and flax rust. *Adv. Genet.* 8:29-54.
9. HEATH, M. C. 1976. Hypersensitivity, the cause or consequence of rust resistance? *Phytopathology* 66:935-936.
10. HEATH, M. C. and I. B. HEATH. 1971. Ultrastructure of an immune and a susceptible reaction of cowpea leaves to rust infection. *Physiol. Plant Pathol.* 1:277-287.
11. JOHNSON, L. E. B.; W. R. BUSHNELL; and R. J. ZEYEN. 1979. Binary pathways for analysis of primary infection and host response in populations of powdery mildew fungi. *Can. J. Bot.* 57:497-511.
12. KIRALY, X.; B. BARNA; and T. ERSEK. 1972. Hypersensitivity as a consequence, not the cause, of plant resistance to infection. *Nature* 239:456-458.
13. LITTLEFIELD, L. J. 1973. Histological evidence for diverse mechanisms of resistance to flax rust, *Melampsora lini* (Ehrenb.) Lev. *Physiol. Plant Pathol.* 3:241-247.
14. LOEGERING, W. G. 1966. The relationship between host and pathogen in stem rust of wheat. *Proc. Int. Wheat Gen. Symp.*, 2nd 1963, *Hereditas*, Suppl. 2:167-177.
15. MARES, D. J. 1979. A light and electron microscope study of the interaction of yellow rust (*Puccinia striiformis*) with a susceptible wheat cultivar. *Ann. Bot.* 43:183-189.

16. MAYAMA, S.; J. M. DALY; D. W. REHFELD; and C. R. DALY.
1975. Hypersensitive response of near-isogenic wheat carrying the temperature-sensitive Sr6 allele for resistance to stem rust. *Physiol. Plant Pathol.* 7:35-47.
17. PERSON, C. 1959. Gene-for-gene relationships in host:parasite systems. *Can. J. Bot.* 37:1101-1130.
18. ROWELL, J. B.; W. Q. LOEGERING; and H. R. POWERS, JR.
1963. A genetic model for physiologic studies of mechanisms governing development of infection type in wheat stem rust. *Phytopathology* 53:932-937.
19. SHARP, E. L. and R. G. EMGE. 1958. A tissue transplant technique for obtaining abundant sporulation of races of *Puccinia graminis* var. *tritici* on resistant varieties. *Phytopathology* 48:696-697.
20. STAKMAN, E. C. 1915. Relation between *Puccinia graminis* and plants highly resistant to its attack. *J. Agric. Res.* 4:193-199.
21. WARD, H. M. 1902. On relations between host and parasite in the bromes and their brown rust, *Puccinia dispersa* Eriksse. *Ann. Bot., Lond.* 16:233-315.

APPENDIX A

Additional Scanning Electron
Microscope Studies of
T. aestivum:P. recondita

Due to constraints on journal article length, an appendix follows which contains additional scanning electron micrographs to support the results of the various chapters of the body of the thesis.

Legends are included on facing pages to describe the micrographs with minimal referral to the text. A table of notations used in the legends is given below.

Host lines:

Thatcher, CI 10003 = TC; Thatcher *6/Exchange RL 6004 =LR

Parasite cultures:

UN01-68A, PR67 = 68A; UN01-68B, PR51 = 68B

Fixation schedules:

Lactophenol:ethanol 1:2, overnight at 25°C = Le; Chloral hydrate, overnight at 25°C = Ch; Standard fixation schedule. (See Chapter I) = Sf

Preparative techniques:

Direct examination of fresh tissue = D; Fixed, dehydrated, sputter coated = F; Resin etch = R; Wax etch = W

These factors will be noted at the end of each legend in the following manner:

Host line: Parasite culture/Days post-inoculation/
Fixation/Preparation/Scale bar length.

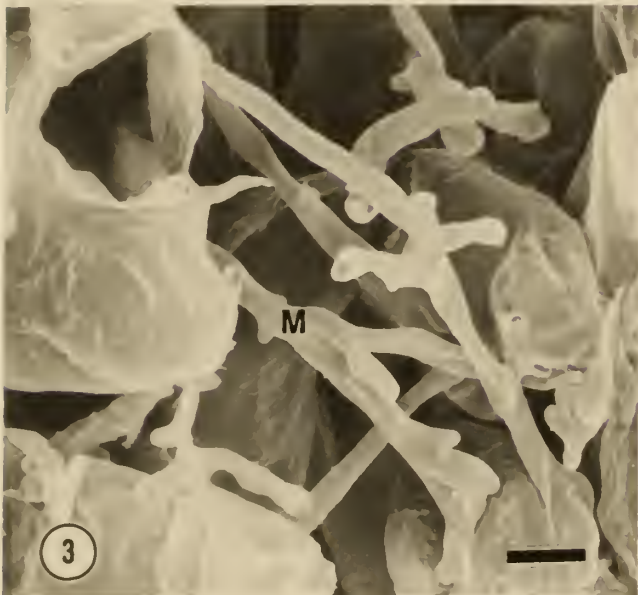
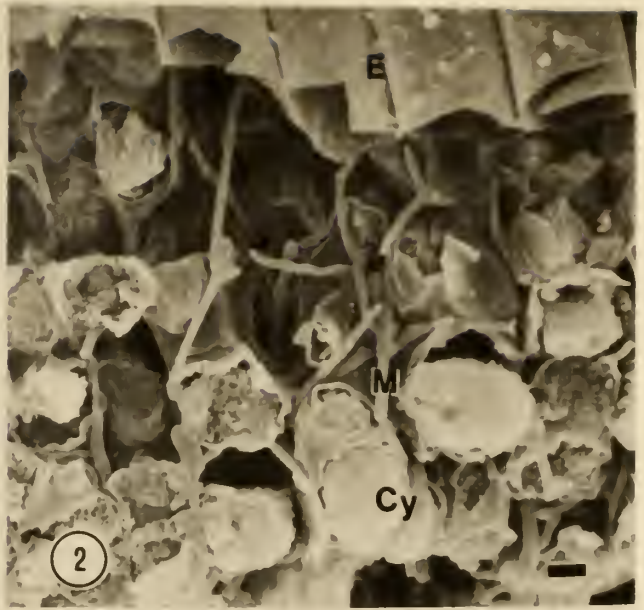
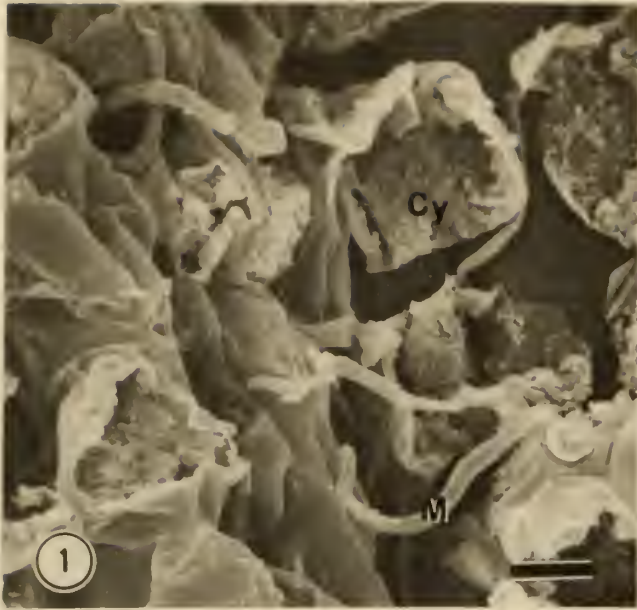


Fig. 1. Intercellular mycelium (M) in tissue fixed in 1:2 lactophenol:ethanol. Note the excessive host cytoplasm (Cy) and the shrinkage of the mycelium. TC:68A/3/Le/F/10um.

Fig. 2. Intercellular mycelium (M) in tissue fixed in chloral hydrate. Note the shrinkage of the mycelium, the excessive host cytoplasm (Cy) and host epidermis E. TC:68A/6/Ch/F/10um.

Fig. 3. Intracellular mycelium (M) in tissue fixed with the standard fixation schedule. Note the absence of shrinkage. TC:68A/14/Sf/F/10um.

Fig. 4. Haustorial mother cell (HMC) with a neck scar (arrow). LR:68A/14/Sf/F/10um.

Fig. 5. Haustorial mother cell showing typical lateral branching behind haustorial mother cells (arrow). TC:68B/3/Sf/R/10um.

Fig. 6. Intracellular mycelium and haustorial mother cell in tissue fixed in 1:2 lactophenol:ethanol. Note that the haustorial mother cell has not shrunken like the intracellular mycelium. TC:68A/6/Ch/F/10um.

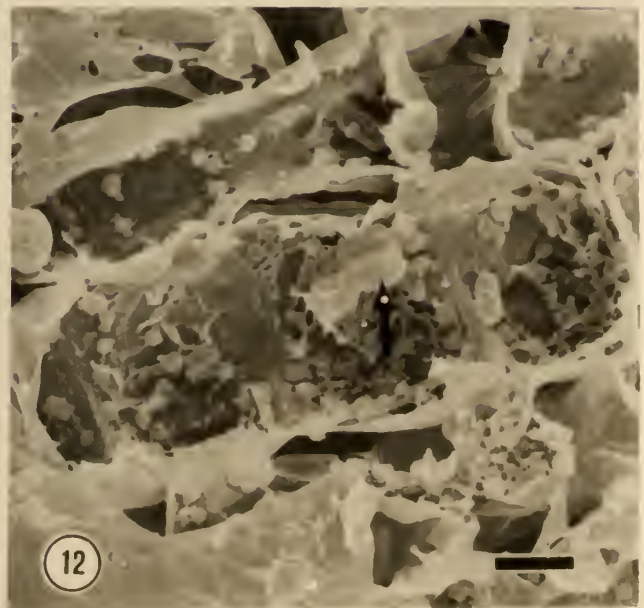
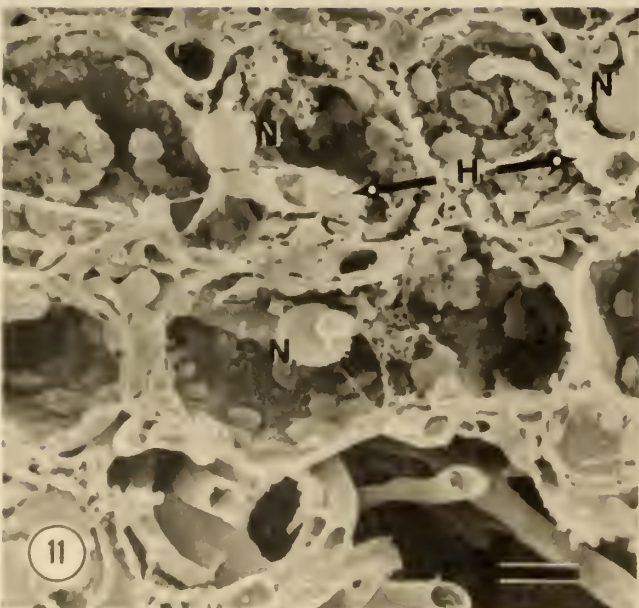
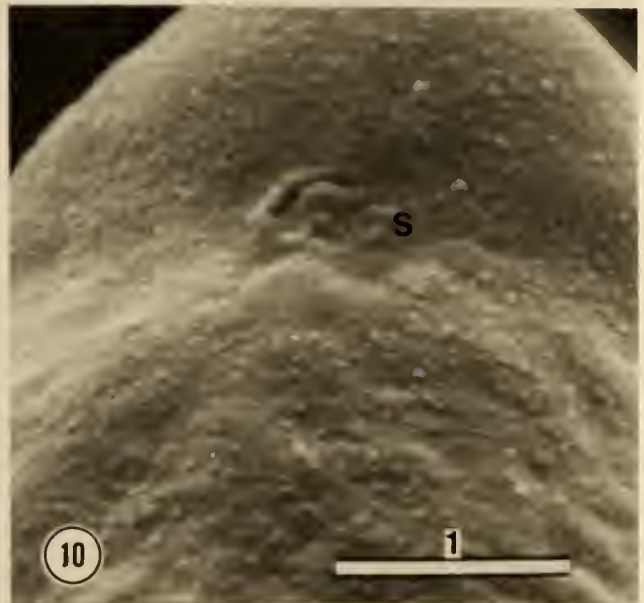
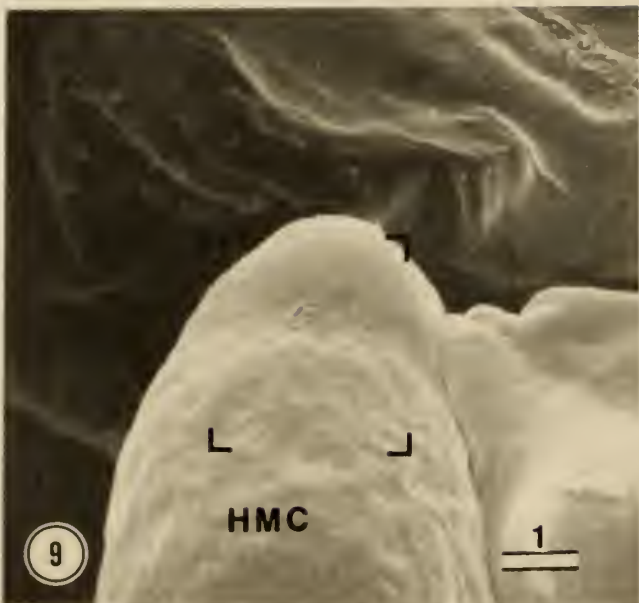
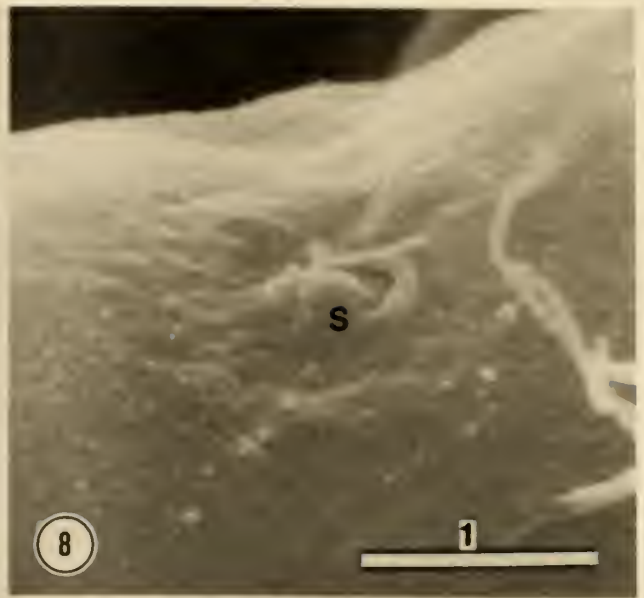
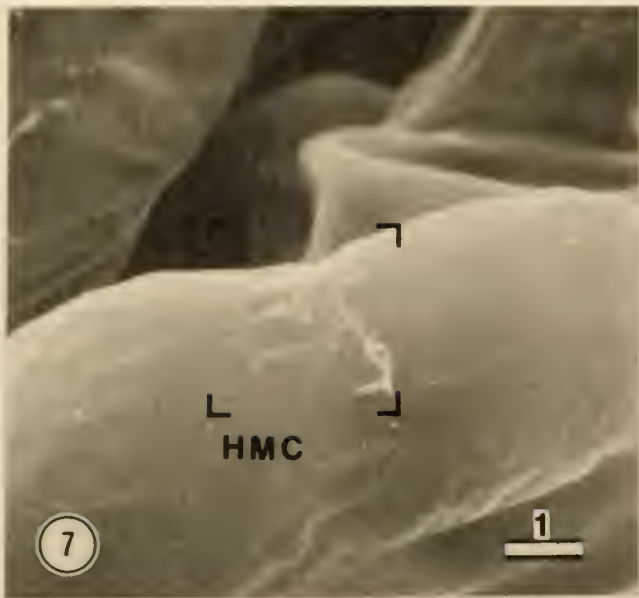


Fig. 7. Haustorial mother cell (HMC) with a neck scar.
TC:68A/14/Sf/F/1um.

Fig. 8. An enlargement of the area in brackets in Fig. 7.
Note the distinct inner and outer cell wall layers at the
site of the neck scar (S). TC:68A/14/Sf/F/1um.

Fig. 9. Haustorial mother cell (HMC) with neck scar.
TC:68A/14/Sf/F/1um.

Fig. 10. An enlargement of the area in brackets in Fig. 9.
Note the outer cell wall layer at the periphery of the neck
scar. TC:68A/14/Sf/F/1um.

Fig. 11. Haustoria (H) at arrows in close proximity to host
nuclei. LR:68A/5/Sf/R/10um.

Fig. 12. Haustorium in close proximity host nucleus.
LR:68A/7/Sf/W/10um.

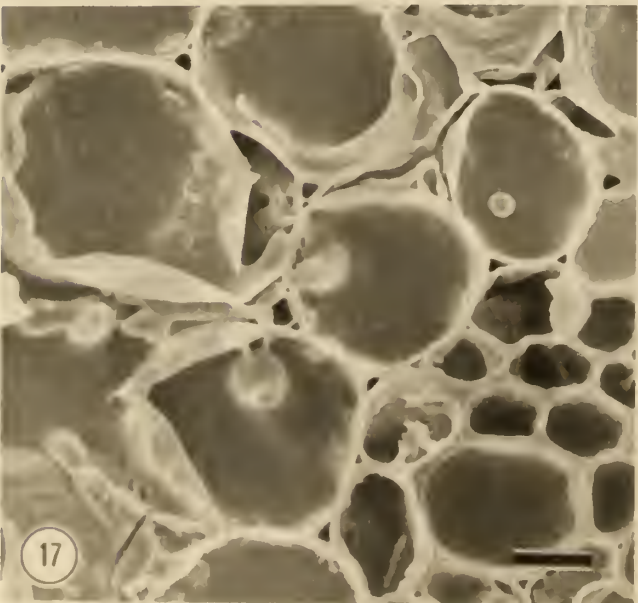
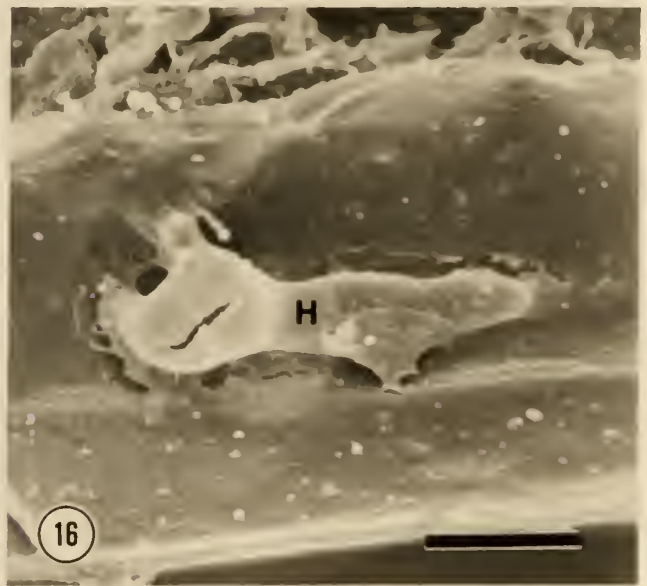
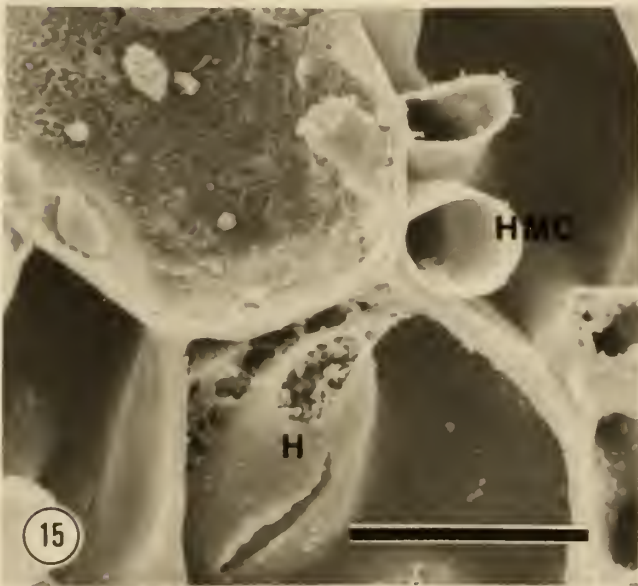
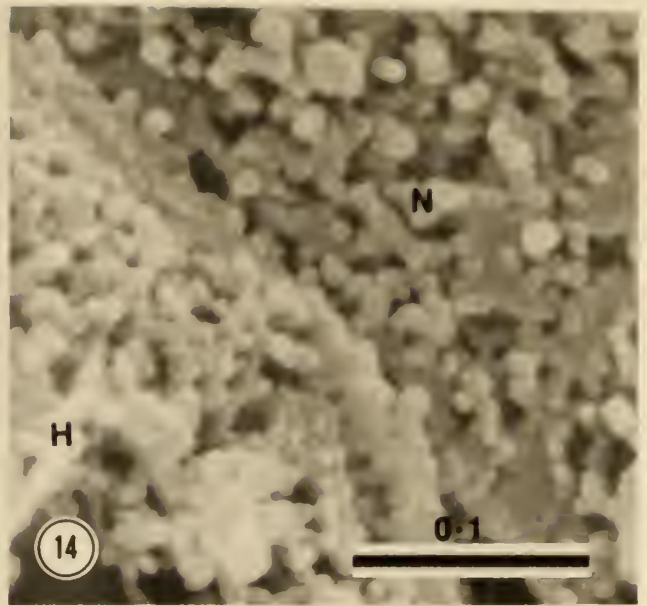
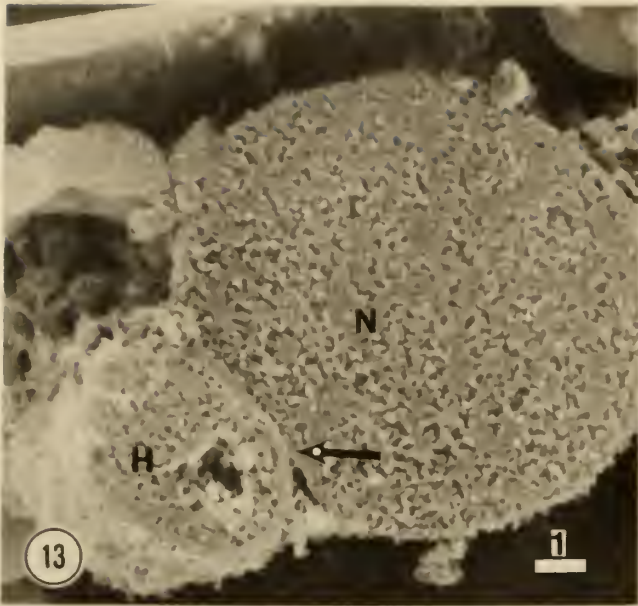


Fig. 13. Haustorium (H) in direct contact with a host nucleus (N). Note the atrophy at the site of contact (arrow). LR:68A/5/Sf/R/1um.

Fig. 14. An enlargement of the site of contact in Fig. 13. LR:68A/5/Sf/R/0.1um.

Fig. 15. A non-median section through a haustorial mother cell (HMC) and haustorium (H). Note the presence of cytoplasm in the haustorium, and relative lack of cytoplasm in the haustorial mother cell. TC:68A/5/Sf/R/10um.

Fig. 16. A haustorium (H) invading a host epidermal cell. TC:68A/5/Sf/R/10um.

Fig. 17. Haustoria invading a host bundle sheath cell. TC:68B/5/Sf/R/10um.

Fig. 18. An enlargement of Fig. 17, showing a capitate haustoria (H) with a small finger-like lobe attached to a haustorial mother cell by a haustorial neck (arrow). TC:68B/5/Sf/R/1um.

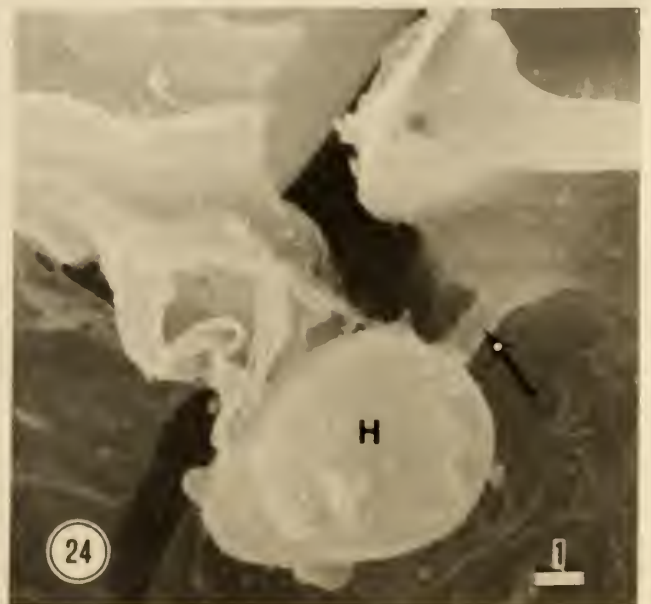
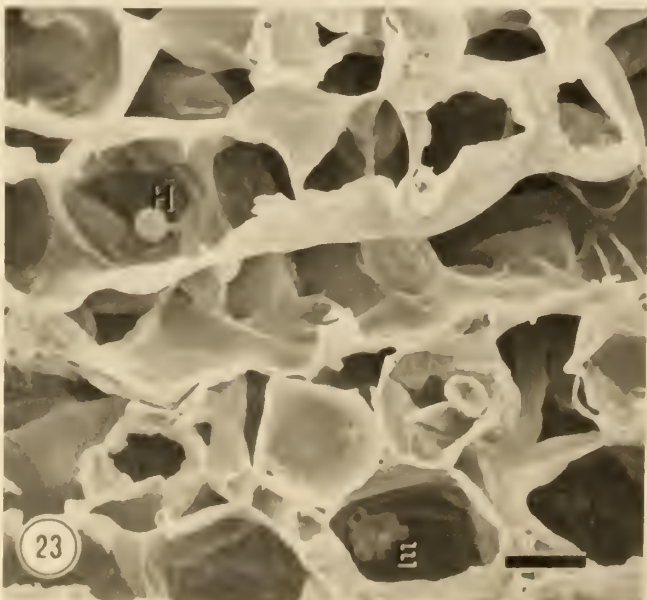
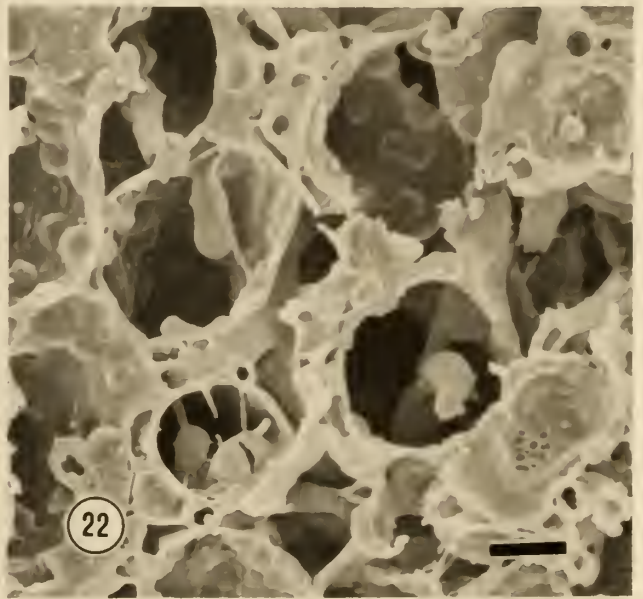
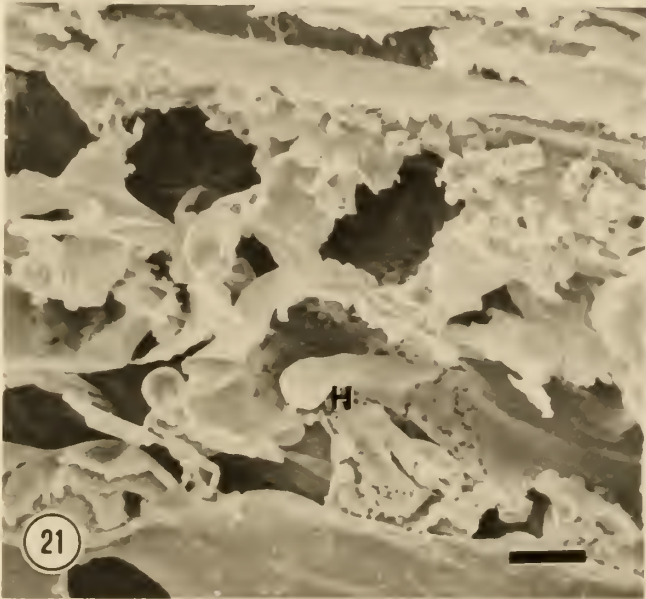
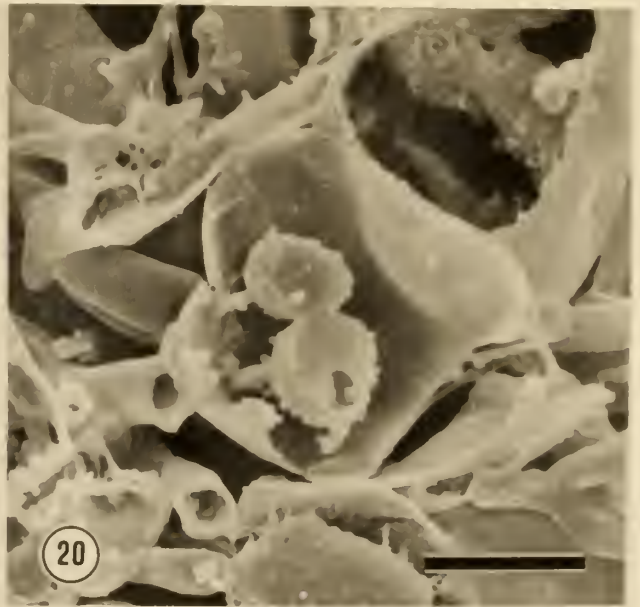
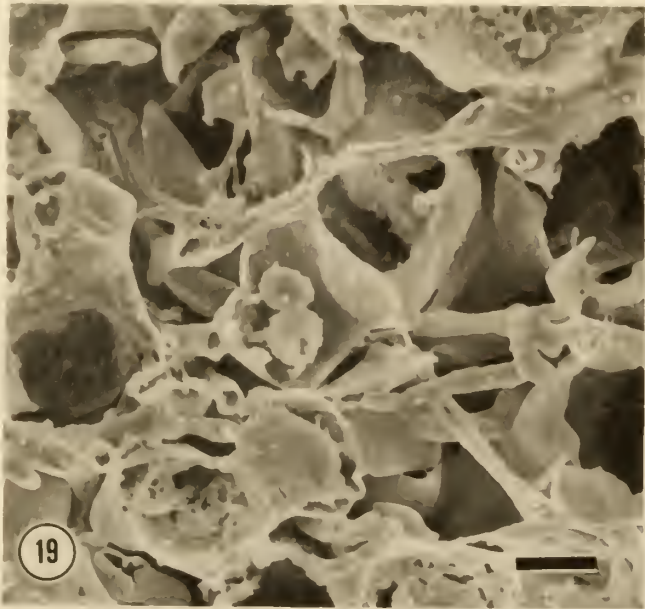


Fig. 19. Two haustoria invading a single host cell.

LR:68B/5/Sf/R/10um.

Fig. 20. An enlargement of Fig. 19. Note the neck connections between the haustoria and the mother cells.

LR:68B/5/Sf/R/10um.

Fig. 21. Haustoria (H) with host plasmalemma intact.

TC:68B/7/Sf/W/10um.

Fig. 22. Several host cells invaded by haustoria.

TC:68B/5/Sf/R/10um.

Fig. 23. Haustoria (H) and a possible encapsulation (E) of a haustorium. LR:68A/7/Sf/W/10um.

Fig. 24. Haustorium (H) and haustorial neck (arrow).

LR:68B/7/Sf/W/10um.

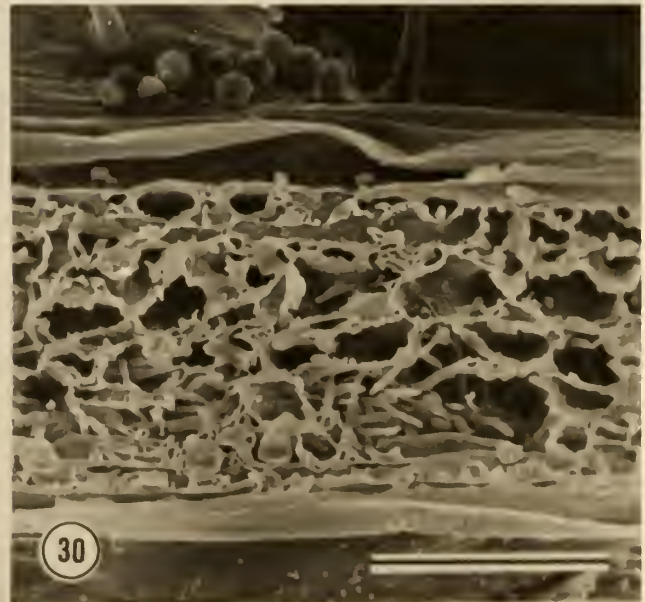
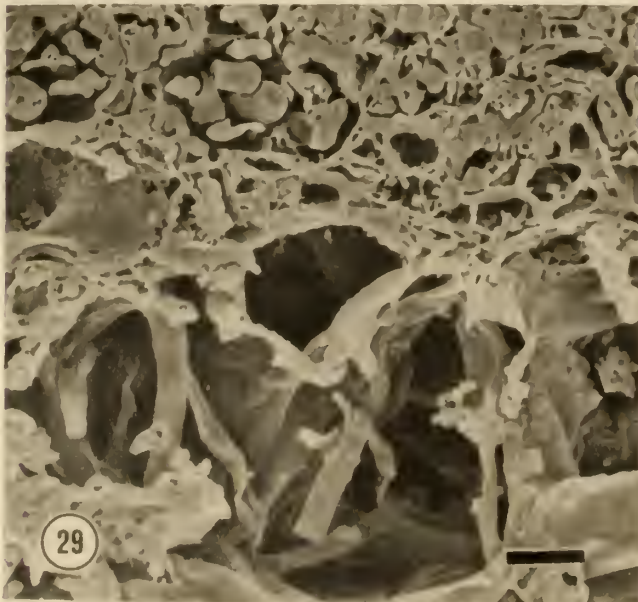
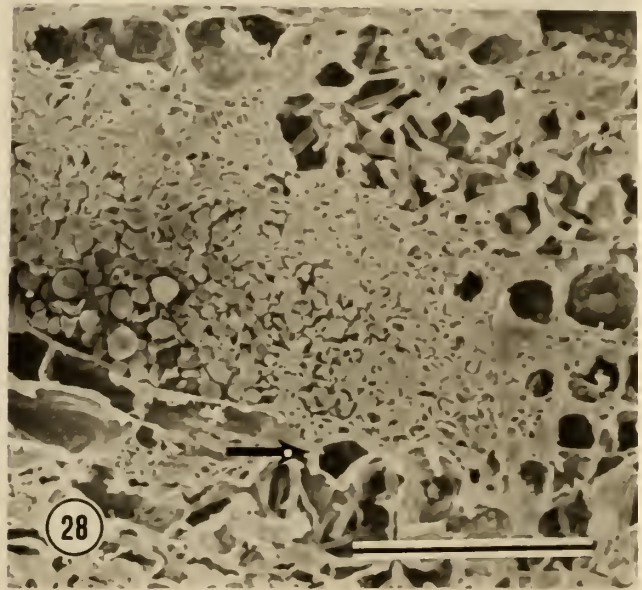
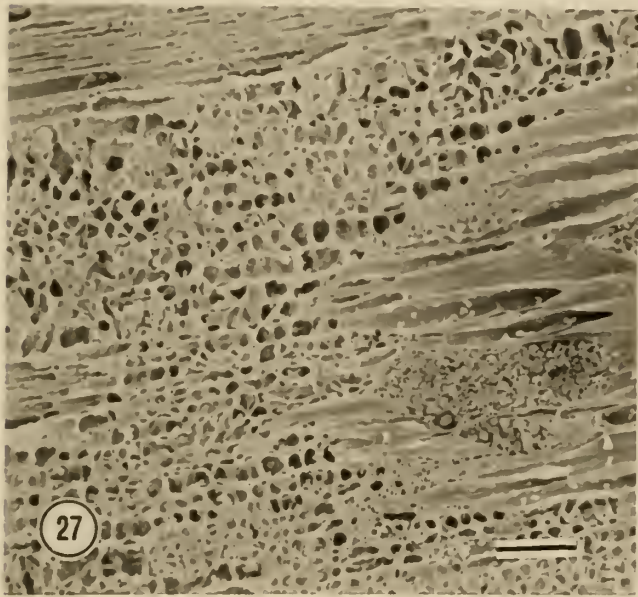
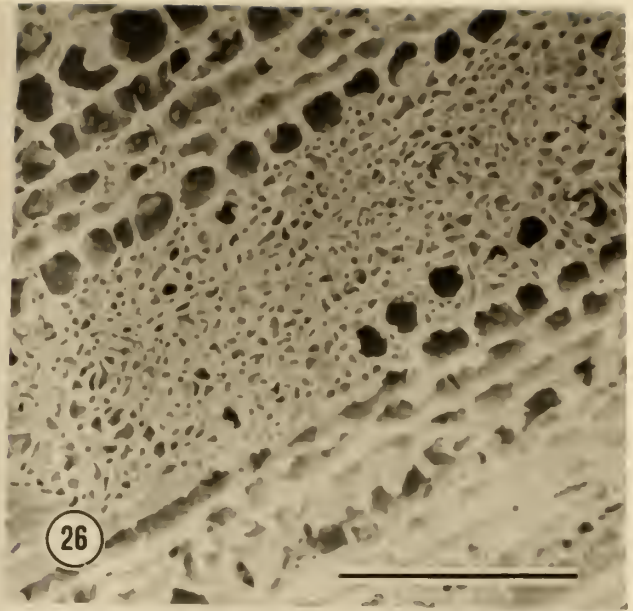
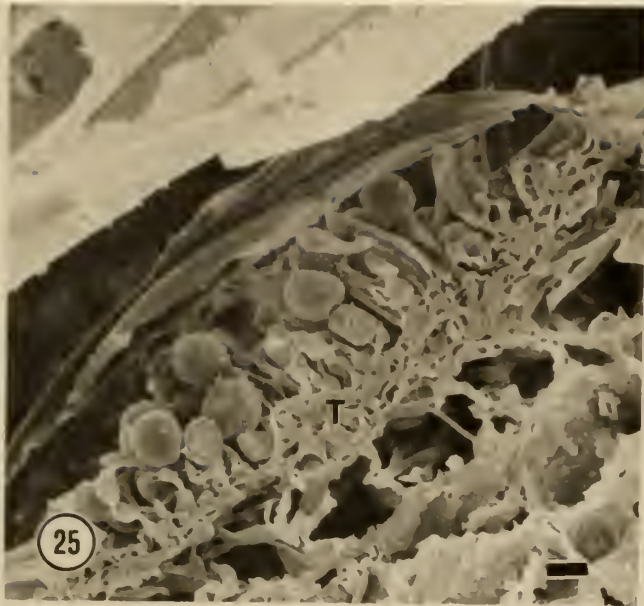


Fig. 25. A developing uredium with urediospores and paraphyses that have arisen from the mycelial thallus (T).
LR:68A/7/Sf/W/10um.

Fig. 26. Sagital section through the thallus beneath a uredium. TC:68B/7/Sf/W/100um.

Fig. 27. Near sagital section through an infected leaf.
LR:68A/7/Sf/W/100um

Fig. 28. Sagital section through the base of a uredium.
TC:68A/7/Sf/W/100um.

Fig. 29. Enlargement of the area pointed to by the arrow in
Fig. 28. TC:68A/7/Sf/W/10um.

Fig. 30. Longitudinal section through a leaf infected with
mycelium. TC:68B/7/Sf/W/100um.

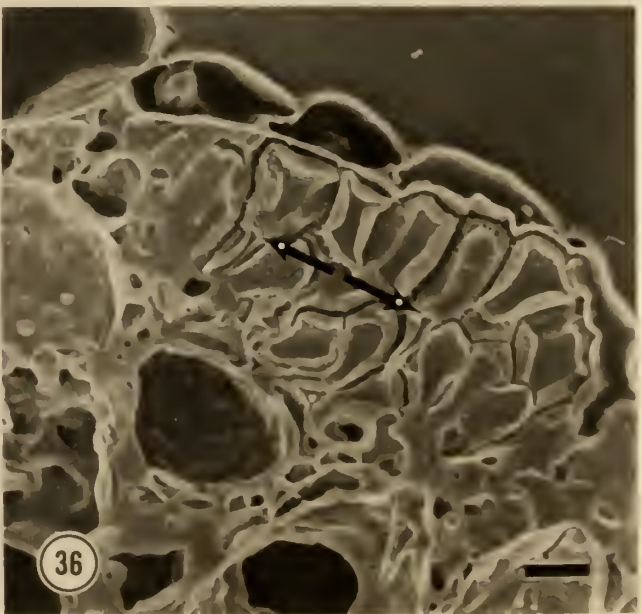
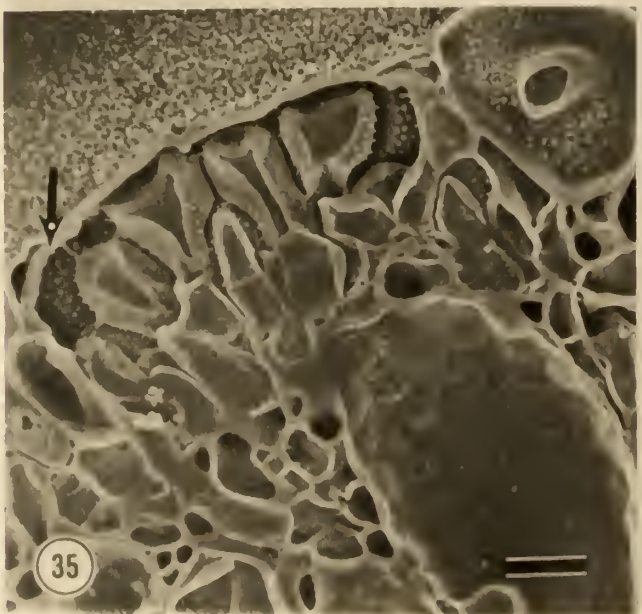
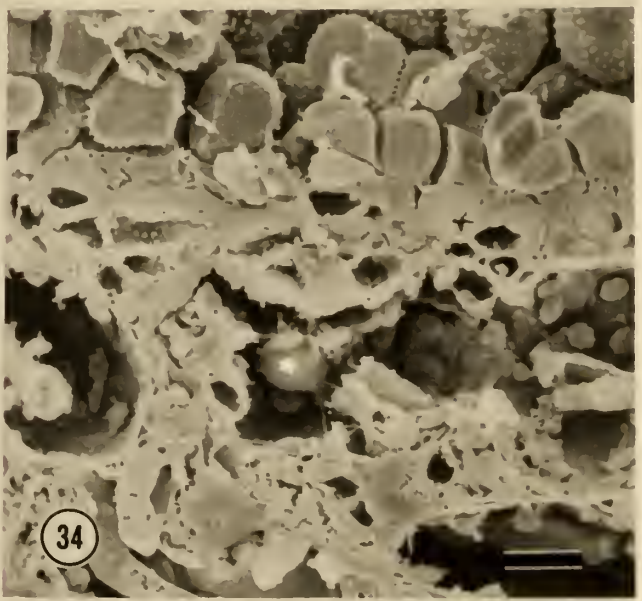
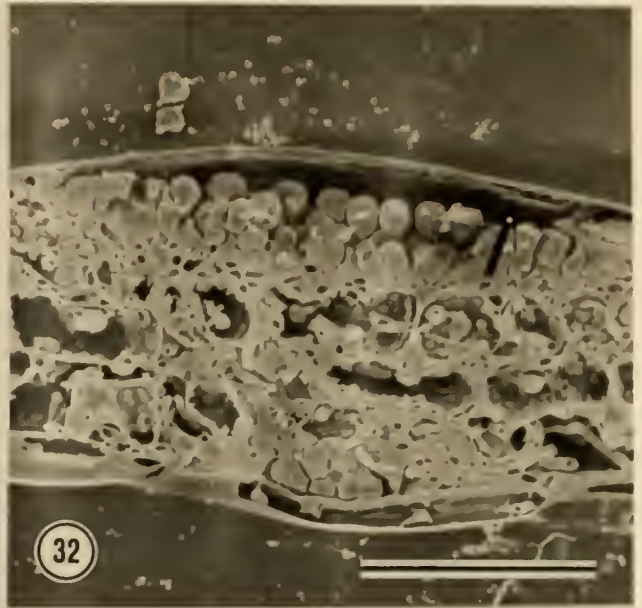
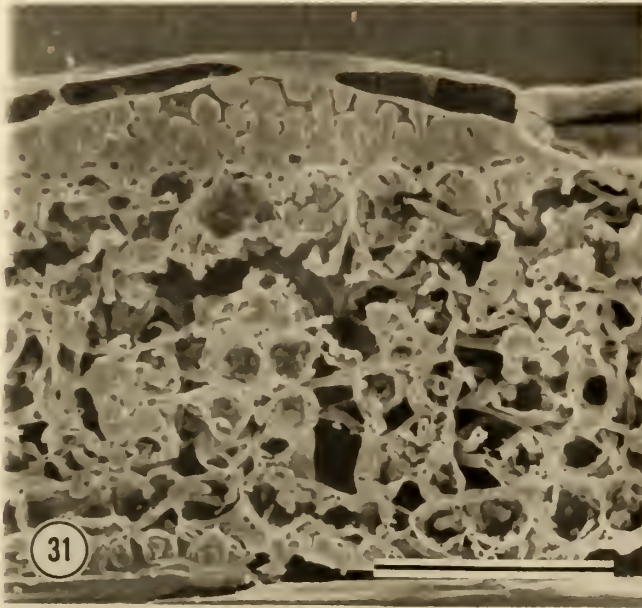


Fig. 31. Longitudinal section through a developing uredium. Note compression of epidermal cells above uredium. TC:68A/5/Sf/R/100um.

Fig. 32. Longitudinal section through a developing uredium. Note the peridium (arrow) below the host epidermis and also the presence of several haustoria close the host nuclei in the bundle sheath cells. A smaller pustule is forming on the adaxial leaf surface. LR:68A/5/Sf/R/100um.

Fig. 33. Longitudinal section through a developing uredium. TC:68A/5/Sf/R/100um.

Fig. 34. An enlargement of Fig. 32. Note the dense cytoplasm in the thallus and developing urediospores. LR:68A/5/Sf/R/100um.

Fig. 35. A transverse section through a uredium. Note the presence of a peridium (arrow) immediately below the host epidermis. TC:68B/5/Sf/R/10um.

Fig. 36. Similar to Fig. 35. Note the formation of a septa (arrows) between urediophores and urediospores. TC:68B/5/Sf/R/10um.

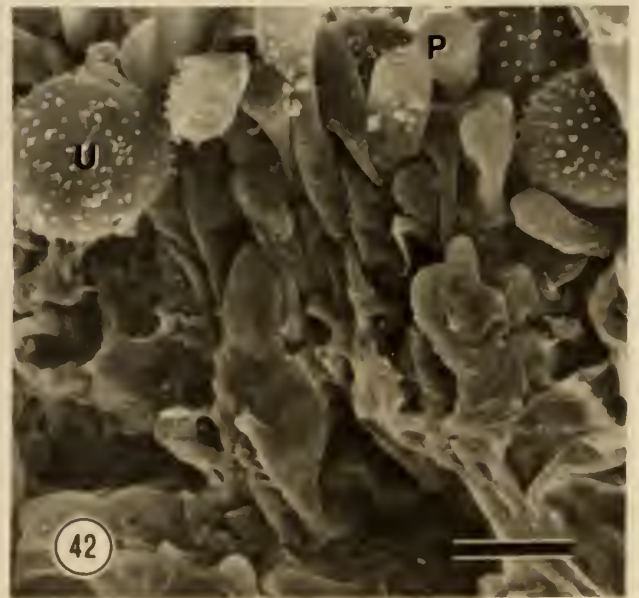
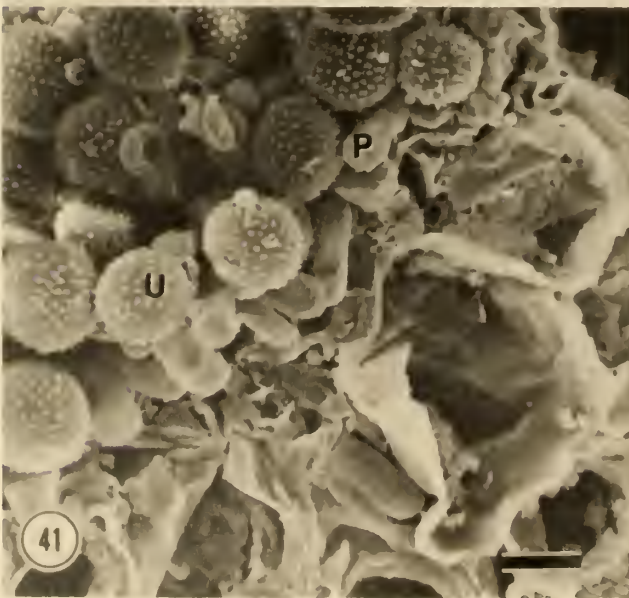
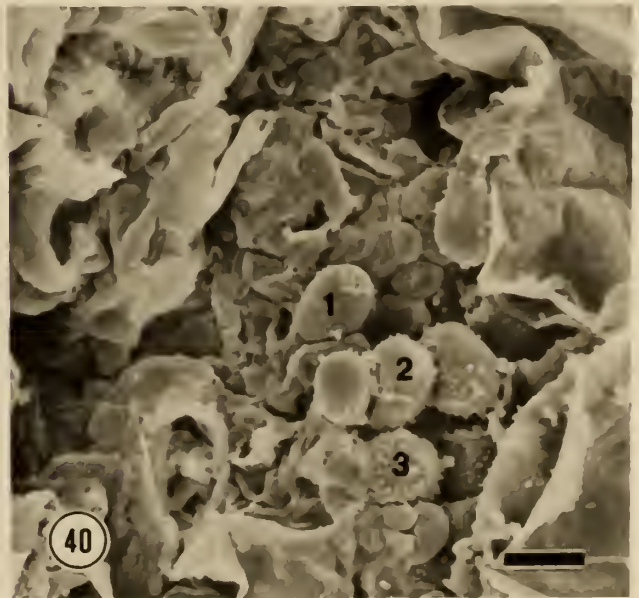
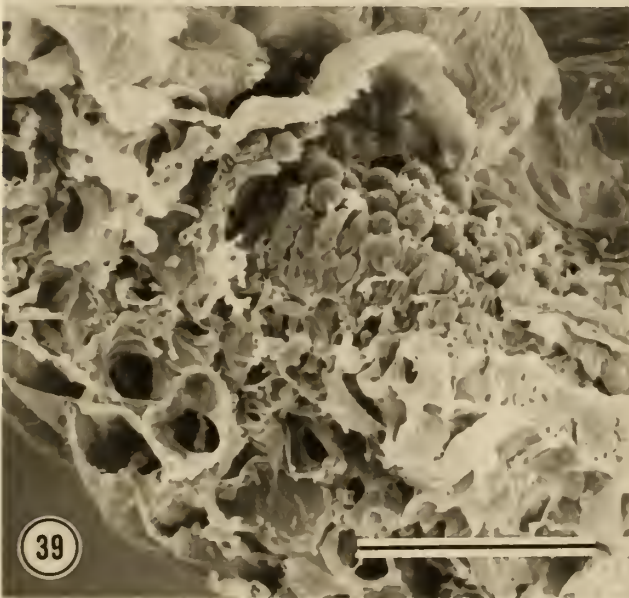
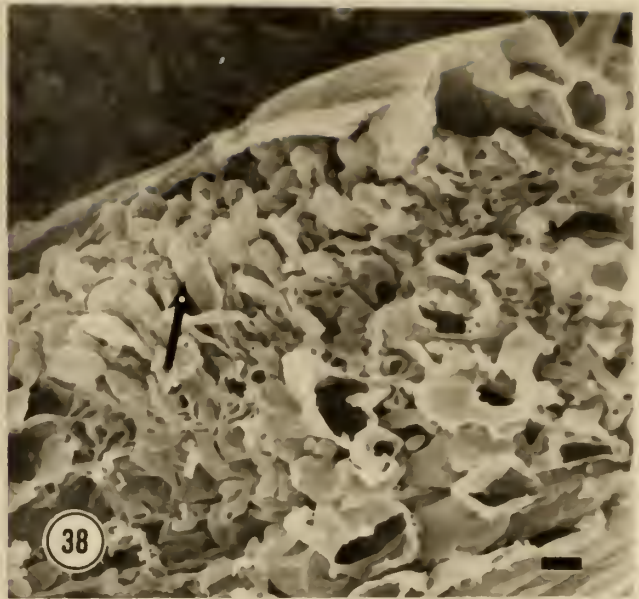
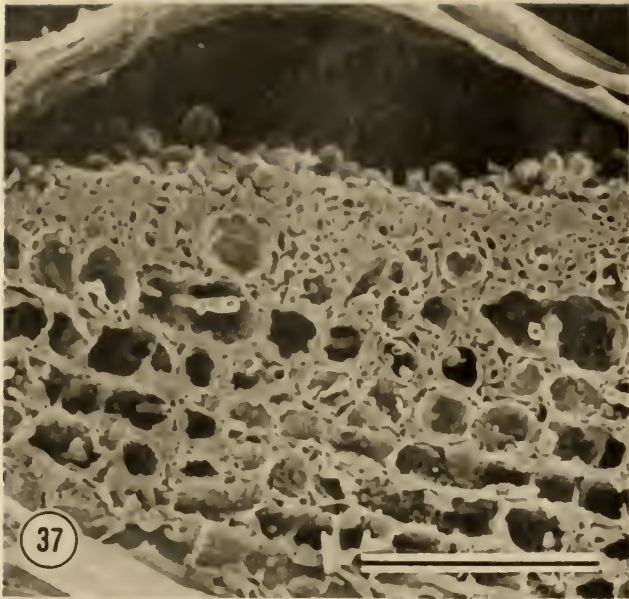


Fig. 37. Longitudinal section through a uredium. Most of the urediospores have been dislodged in handling. Note the remnants of the peridium, the extensive mycelial thallus, and host cells invaded by haustoria. TC:68A/7/Sf/W/100um.

Fig. 38. Free hand section through a uredium. Note the various stages of urediospore development and the elongated paraphyses (arrow). LR:68B/14/Sf/F/10um.

Fig. 39. Similar to Fig. 38. Note the germ tube pores in the fully developed urediospores. LR:68A/14/Sf/F/100um.

Fig. 40. Similar to Fig. 38. Note the stages in urediospore development. TC:68B/5/Sf/F/10um.

Fig. 41. Similar to Fig. 38. TC:68B/7/Sf/F/10um.

Fig. 42. Similar to Fig. 38. Note the development of the paraphyses. LR:68A/7/Sf/W/10um.

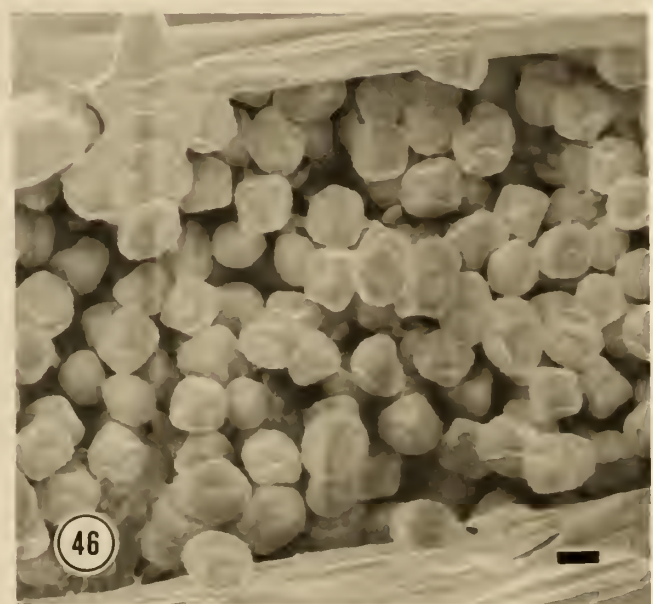
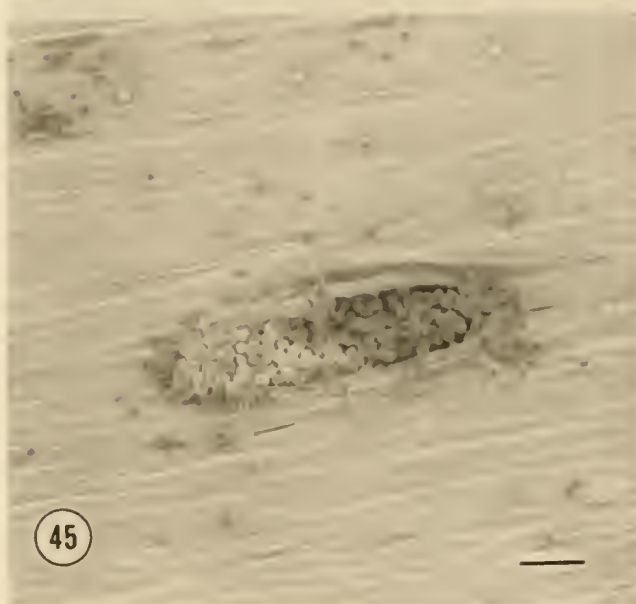


Fig. 43. A typical high infection type uredium. Note the host trichomes. TC:68A/14/Sf/F/100um.

Fig. 44. A high infection type uredium that has just begun to break the host epidermis. TC:68B/7/Sf/W/100um.

Fig. 45. Fresh uncoated tissue. Note the light color of the epidermis due to a crystalline-wax lattice as compared to Fig. 44 where the lattice was removed during critical-point drying. Charging is also present on urediospores because of the lack of metallic-coating. TC:68A/14/-/D/100um.

Fig. 46. An enlargement of Fig. 45. Urediospores appear collapsed from high vacuum. TC:68A/14/-/D/100um.

Fig. 47. Urediospore development. TC:68A/14/Sf/F/10um.

Fig. 48. Urediospore development. Note the progression of spore development, and paraphyses. TC:68B/5/Sf/F/10um.

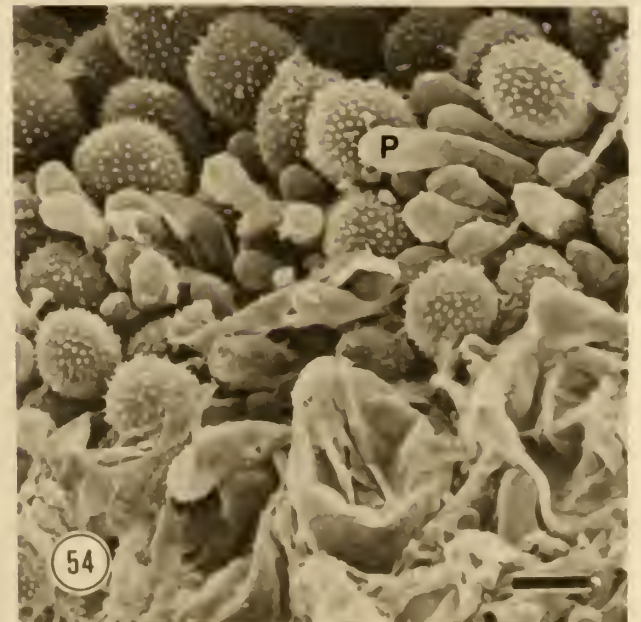
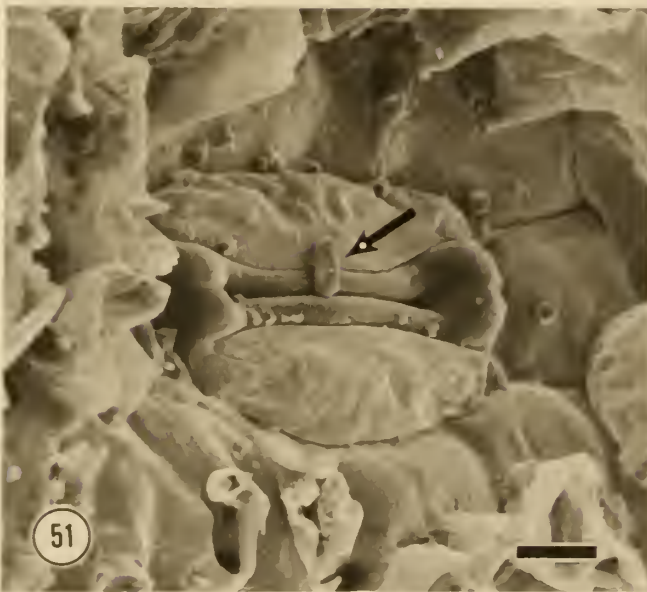
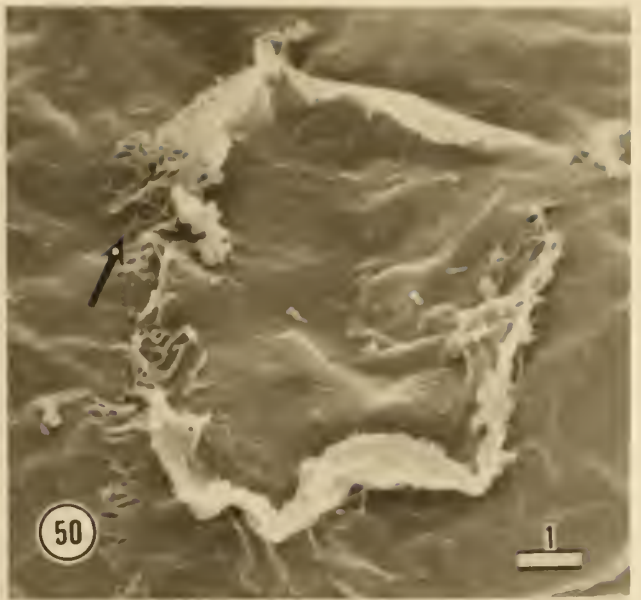
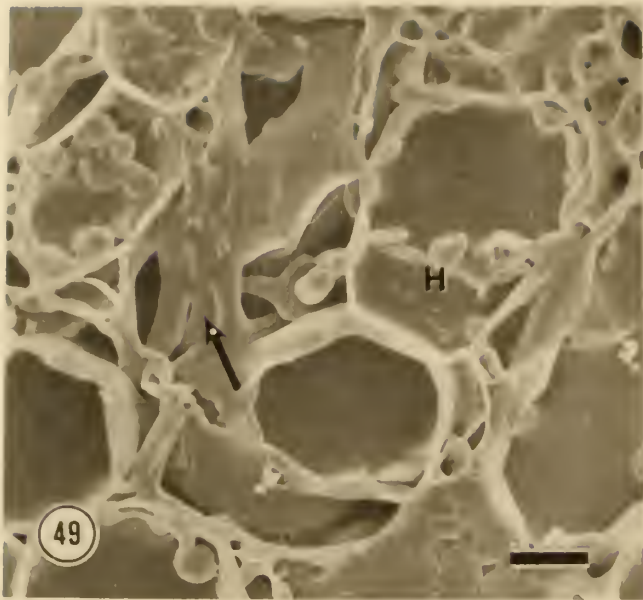


Fig. 49. Possible hypal fusion (arrow) and haustoria (H). Hypal fusion (anastomosis) may permit transfer of nuclei from one hypae to another. TC:68B/5/Sf/R/10um.

Fig. 50. Possible site of contact of haustorial mother cell with host mesophyll cell. Note the fibrillar matrix (arrow) at the margin of contact. LR:68A/14/Sf/F/1um.

Fig. 51. View of a host stoma from the substomatal chamber with a possible substomatal vesicle (arrow). TC:68B/7/Sf/W/10um.

Fig. 52. Similar to Fig. 51, with a definite strand of intracellular mycelium (M) next to the host guard cells (GC). TC:68B/7/Sf/W/10um.

Fig. 53. Uredium development in low infection type complete with urediospores, and paraphyses. LR:68B/14/Sf/F/10um.

Fig. 54. Uredium development in high infection type including urediospores and paraphyses (P). TC:68B/7/Sf/F/10um.

APENDIX B

Ultraviolet Fluorescent Microscopy of

T. aestivum:P. recondita

Tissue was prepared for examination with ultraviolet fluorescence microscopy by a modification of the method of Rohringer et al. (Phytopathology 67:808-810). The modification was the substitution of Tinopal UNPS for Calcofluor as the optical brightener. This method permitted observation of the entire infection cycle except for development of haustoria which could not be visualized by this technique. Necrotic host cells could be observed without the use of an optical brightener; in fact, this autofluorescence was quenched after treatment in Tinopal UNPS. This method had the advantage of permitting observation of internal infection structures without sectioning the tissue, and also permitted quantification of the amount of tissue infected by fungal mycelium.

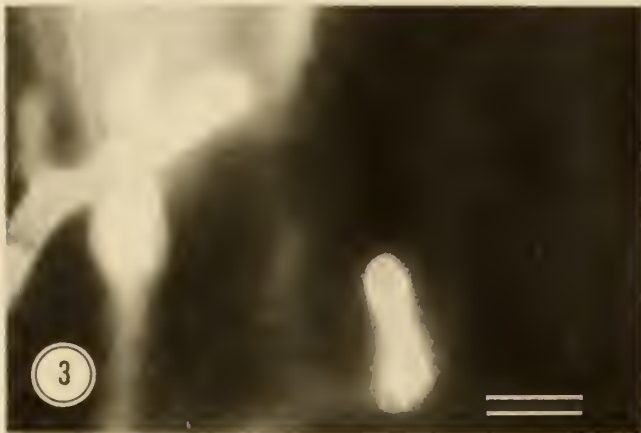


Fig. 1. Primary infection of host occurred when urediospores (U) developed a germ tube that contacted a host stomate, and formed appressoria (A) with finger-like attachments to the host stomatal guard cells. Scale bar = 10um.

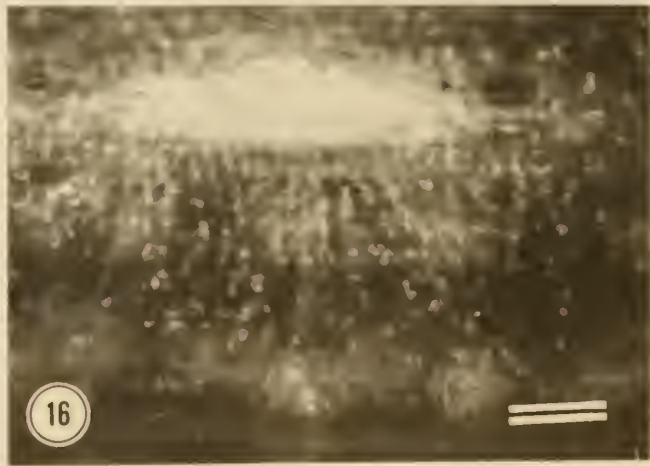
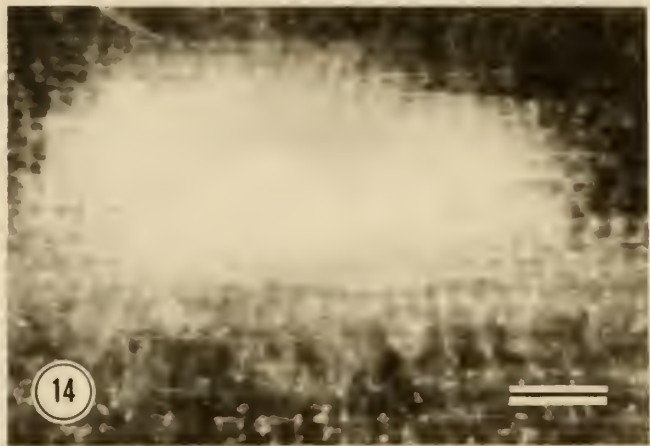
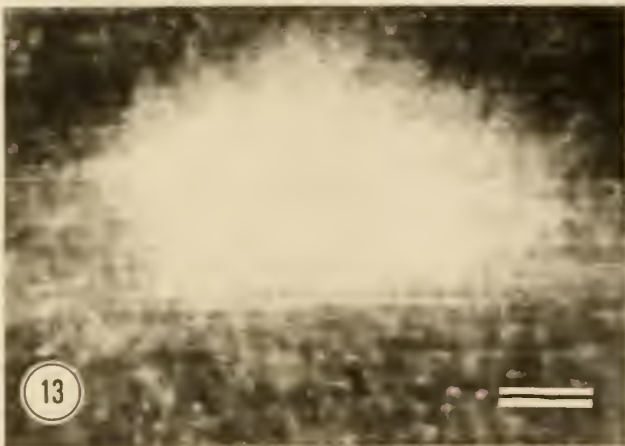
Fig. 2. A substomatal vesicle and first stages of intercellular mycellium formation. Scale bar = 10um.

Fig. 3 and Fig. 4. Intercellular mycelia and developing haustorial mother cells delimited from the mycelia by a distinct septa (arrow). Haustoria were not visible with U. V. fluorescence. The haustorial mother cells fluoresced with greater intensity than intercellular mycelia. Scale bar = 10um.

Fig. 5 and Fig. 6. The colony perimeter extensively invaded by mycelium and haustorial mother cells. Scale bar = 10um.

Fig. 7. A necrotic host cell that autofluoresced without addition of Tinopal UNPS stain. Scale bar = 10um.

Fig. 8. The same necrotic cell as Fig. 7 viewed with phase contrast microscopy indicating that the necrosis was due to mechanical damage rather than infection.



Figs. 9 through 12. Autofluorescence of necrotic host cells infected with P. recondita. Such necrotic cells were noted in all four infection types, but more frequently in the low infection type combination (LR:68B). Scale bar = 10um.

Figs. 13 through 16. Infection sites after staining in Tinopal UNPS. The area of infection of the various infection types could be determined with this method. (See Table 1.) Scale bar = 100um.

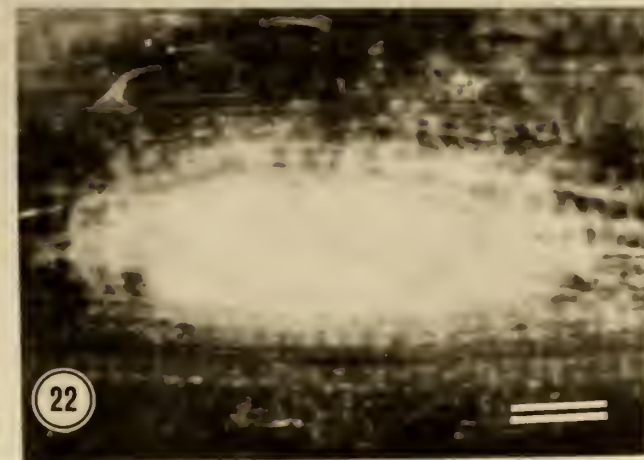
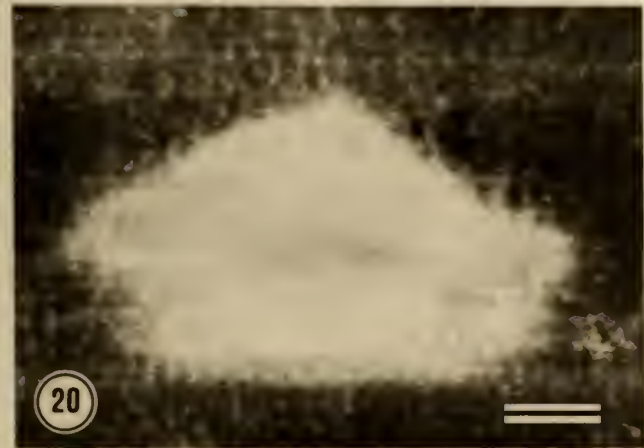
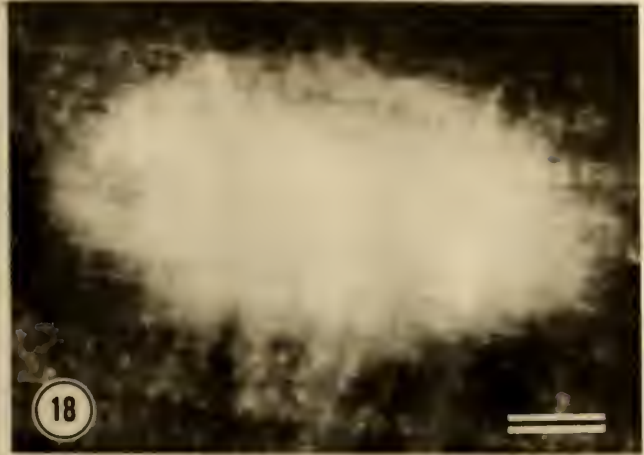


Fig. 17. An example of a low infection type in which the mycelium development has been extremely retarded. Note the bright fluorescence of the substomal vesicle at the lower center of the figure. Scale bar = 10um.

Figs. 18 through 22. Additional examples of colonization of host tissue by P. recondita as seen with U. V. fluorescence. Scale bar = 100um.

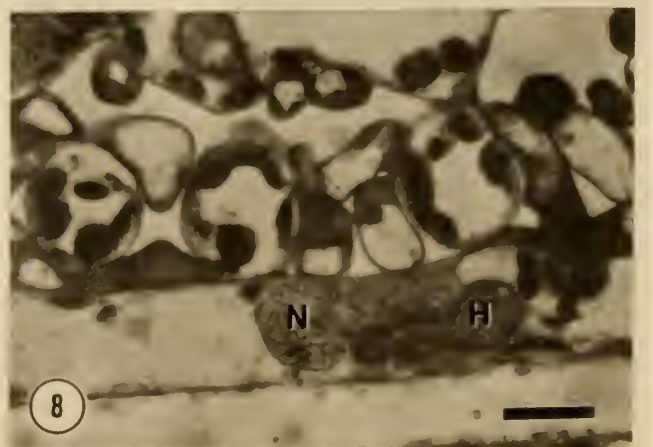
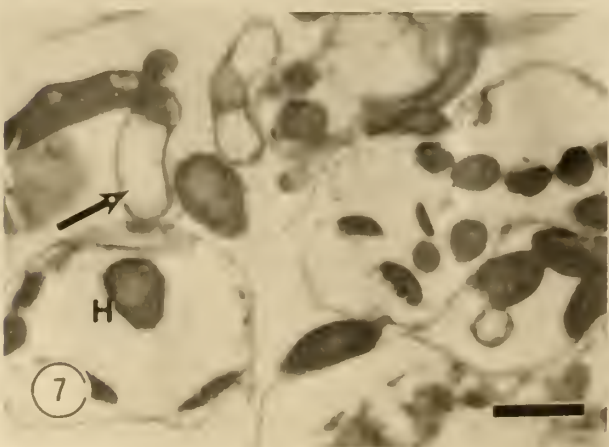
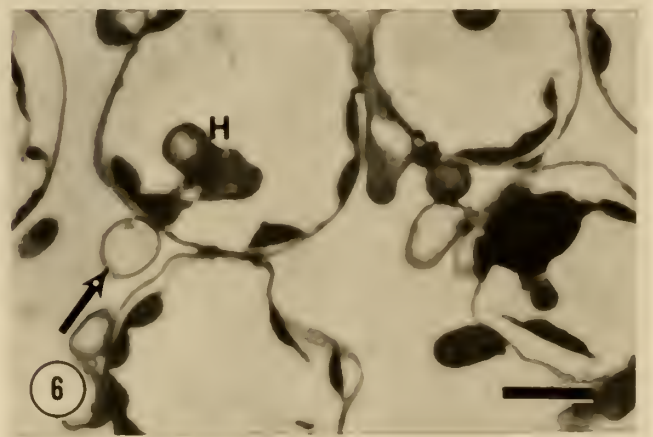
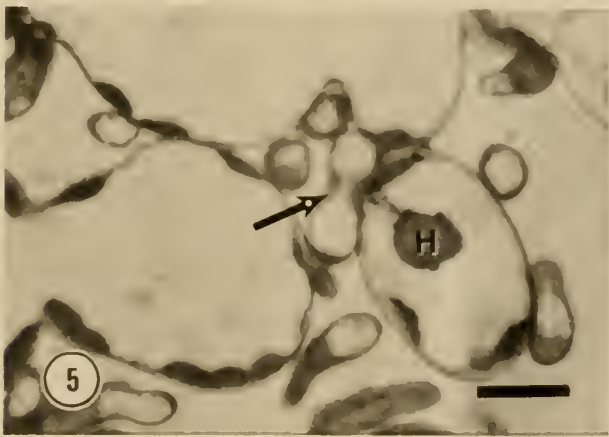
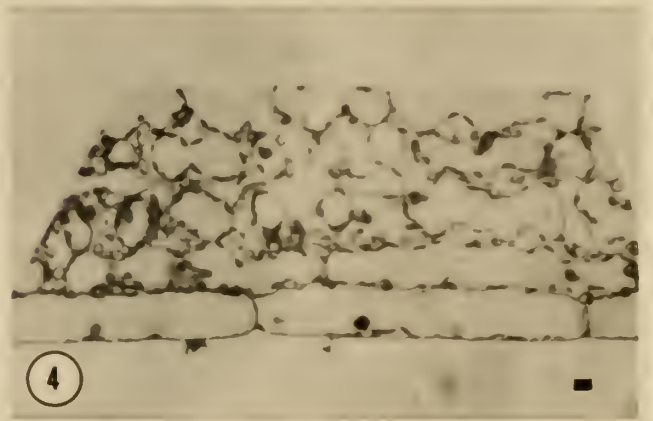
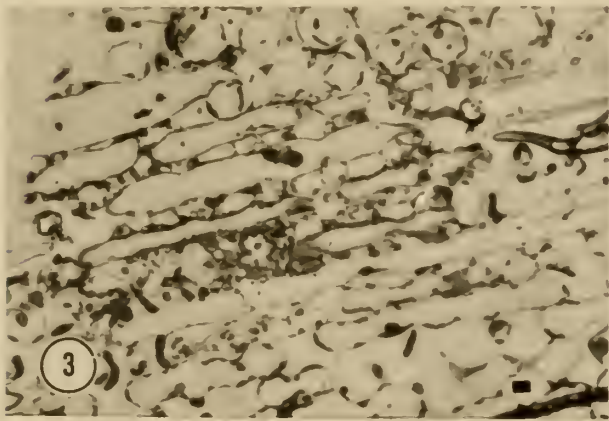
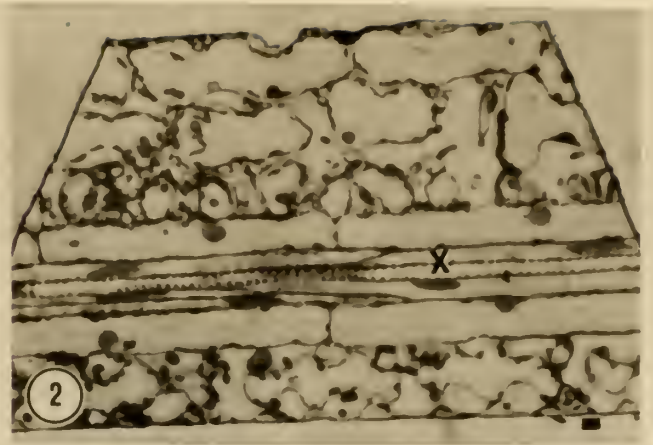
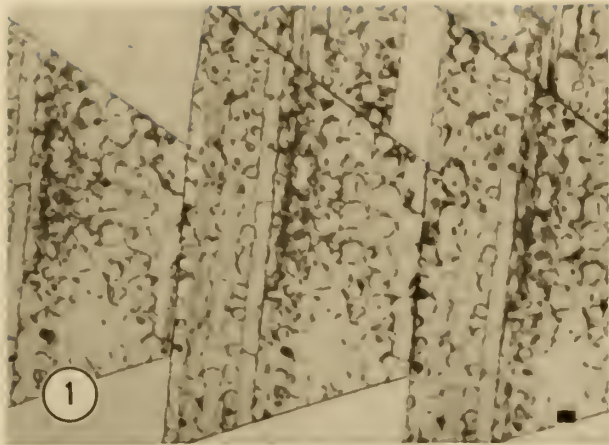
Table No. 1
 Mean Area¹ of Infected Tissue as Determined
 by Ultraviolet Fluorescence

Host : Parasite	Mean Area of Infection (m.m. ²)
LR : 68A	1.6
LR : 68B	0.3
TC : 68A	2.4
TC : 68B	3.1

¹Mean area of infection was determined by the formula $A = (\pi/4) \cdot L \cdot W$, where L and W are the maximal length and width of infection hyphae 14 days after inoculation with urediospores. Seven random infection sites were measured for each host:parasite combination.

APPENDIX C

Light Microscopy of
T. aestivum:P. recondita



Figs. 1 through 8 are thick (10 um) sections of tissue fixed and dehydrated by the standard schedule and embedded in Spurr's low viscosity epoxy resin. The host line Thatcher *6/Exchange, with Lrl0, and parasite culture UN01-68B, with Lpl0, 108 hr after inoculation are represented in all cases. All sections were stained in 1% alkaline toluidine blue prior to observation. The scale bar represents 10 um in all cases.

Fig. 1. Serial sections of tissue extensively infected with fungal mycelia.

Fig. 2. A section through the vascular bundle; with xylem cells (X), phloem, bundle sheath and mesophyll cells. The bundle sheath and mesophyll cells are heavily infected.

Fig. 3 and Fig. 4. Sagittal sections through infected tissue.

Figs. 5 through 7. High magnification (100x objective) of host cells infected with haustoria (H) and their adjacent haustorial mother cells (arrow).

Fig. 8. A haustorium (H) in contact with a host nucleus (N) in a host bundle sheath cell.

APPENDIX D

Transmission Electron Microscopy of

T. aestivum:P. recondita

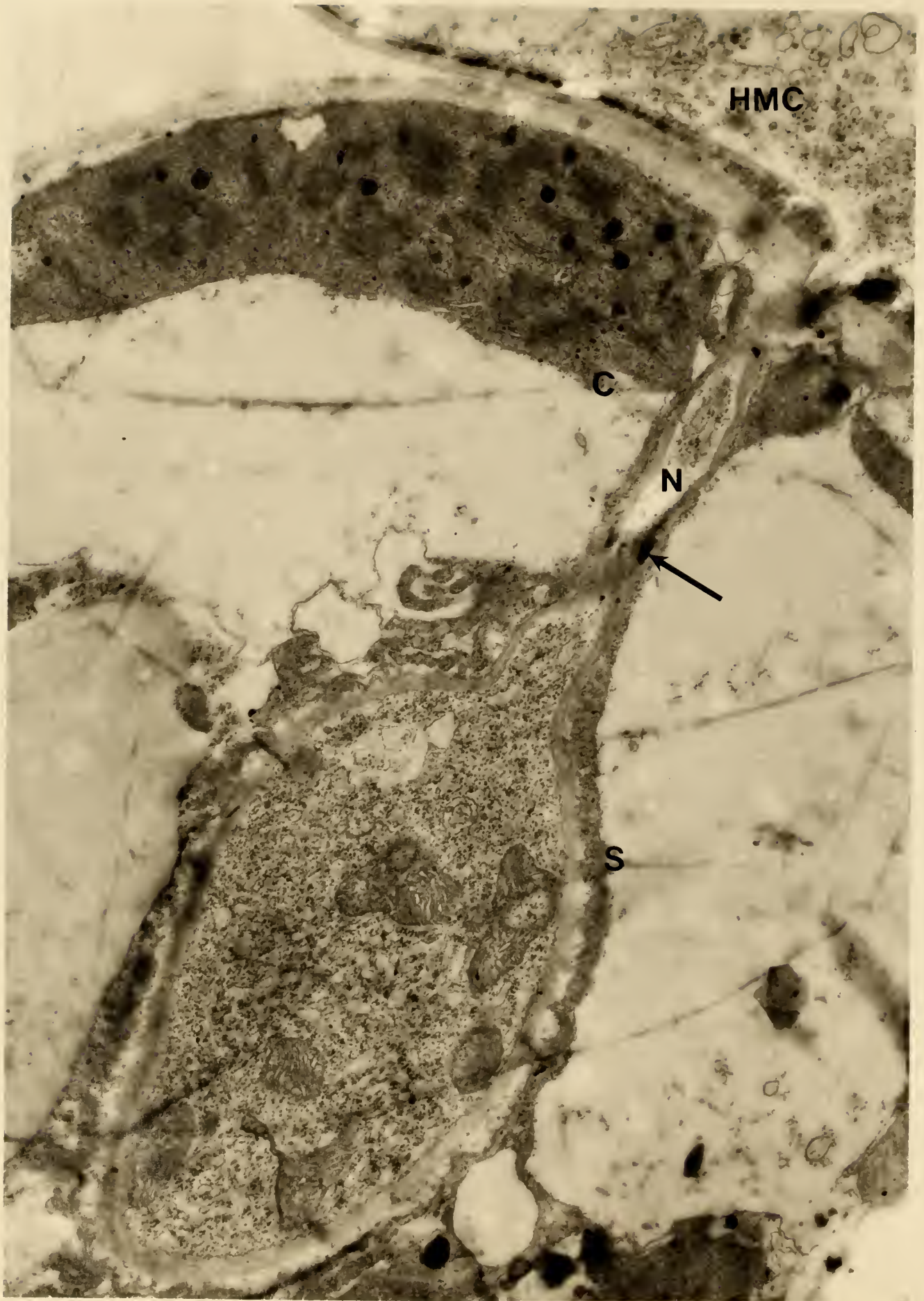


Fig. 1. A transmission electron micrograph through the host:parasite interface that is present in host cell invasion by fungal haustoria. The haustorial mother cell (HMC) is connected to a haustorium (H) by a narrow neck (N). Note the two dark staining areas in the cell wall of the neck (arrow). Also note the host plasmalemma invagination to form a sheath (S) around the haustorium. The cytoplasm inside the haustorium contains mitochondrion and other organelles, while the cytoplasm in the haustorial mother cell is dispersed. A host chloroplast (C) is also present.

SCANNING ELECTRON MICROSCOPE OBSERVATIONS OF
THE TRITICUM AESTIVUM:PUCCINIA
RECONDITA ASSOCIATION

by

DENNIS BLAKE COOPER

B.S., Biology, University of Southern Colorado, 1975

B.S., Chemistry, University of Southern Colorado, 1975

AN ABSTRACT OF

A MASTER'S THESIS

submitted in partial fulfillment of the

requirements for the degree

MASTER OF SCIENCE

Department of Plant Pathology

KANSAS STATE UNIVERSITY
Manhattan, Kansas
1979

ABSTRACT

This investigation of T. aestivum:P. recondita has included an evaluation of techniques applicable to studying this and other host:parasite associations with the scanning electron microscope, the description of the ultrastructural development of the association and the modifications in the ultrastructural development associated with a specific gene for low reaction. Specific conclusions are drawn about each of these areas in the discussion sections of the respective chapters. Each of the methods evaluated proved useful in observation of some portion of the disease cycle, and had advantages and disadvantages with respect to the other methods. The wax-embedding technique was the most useful method for this particular situation. The ultrastructural development of the entire infection cycle was observed with the scanning electron microscope including: primary infection of the host by urediospores, development of intercellular mycellium and haustorial mother cells, formation of haustoria and their relationl to host organelles, and the development of a mycellial thallus prior to uredium formation and the subsequent sporulation phase. The findings of this paper are similar to those reported in other closely related host:parasite associations by other investigators. A quadratic check was used to study the ultrastructural changes associated with the Lr10 gene for

reaction. Three high infection type associations and one low infection type association were produced when two lines of wheat were inoculated with two cultures of P. recondita urediospores. Urediospore germination through formation of haustorial mother cells was similar in all four host:parasite combinations. The development of haustoria was the major histopathological difference noted in the infection types. Haustoria in the high types were typically elongate, while those in the low type were frequently capitate, or capitate with finger-like lobes. Occasionally haustoria in associations where the host had Lr10 were encased by an apposition; this may constitute the 'dimorphic immune response' that has been postulated by Heath and Heath to be active in other host:parasite associations. Other differences in the infection type were largely quantitative in nature, with the low type producing less mycelia and fewer urediospores than the high types. These factors implied that the hypersensitive response may not be the primary determinant of low infection type, with the gene pair tested. The importance of the hypersensitive response in this and other host:parasite associations is not, however, discounted. Additional observations of the T. aestivum:P. recondita association made with the scanning electron microscope, ultraviolet fluorescence, light, and transmission electron microscope are reported in appendices to the body of the thesis.

